ABSTRACT

KOSCH, JENS CARL DIETER. Sampling Impacts the Assessment of Tooth Growth and Replacement Rates in Archosaurs: Implications for Paleontological Studies. (Under the direction of Drs Lindsay Zanno and Mary Schweitzer).

Dietary habits in extinct species cannot be directly observed; thus, in the absence of extraordinary evidence, the dietary ecology of extinct species must be reconstructed with a combination of morphological proxies. Such proxies often include information on dental organization and function such as tooth formation time (TFT) and replacement rate (TRR). In extinct organisms, TFT and TRR are calculated, in part via extrapolation of the space between incremental lines in dental tissues representing daily growth (von Ebner Line Increment Width; VEIW). Tooth formation times and replacement rates in extinct species are becoming regularly calculated; however, to date, little work has been conducted testing assumptions about the primary data underpinning these calculations, specifically, the potential impact of differential sampling and data extrapolation protocols. To address this, we tested a variety of intradental, intramandibular, and ontogentic sampling effects on calculations of mean VEIW, TFT, and TRR using histological sections and CT reconstructions of a growth series of three specimens of the extant archosaurian *Alligator mississippiensis*.

We find transect position within the tooth and orientation with respect to VELs to have the greatest impact on calculations of mean VEIW—a maximum number of VEIW measurements should be made as near to the central axis as possible. Measuring in more crowded regions of the tooth off the central axis can reduce mean VEIW by 36%, causing inflated TFT calculations. We find little demonstrable impact to calculations of mean VEIW from the practice of subsampling along a transect, or from using mean VEIW derived from one portion of the dentition to extrapolate TFT and TRR for other regions of the dentition. Subsampling along transects contributes only minor variation in mean VEIW calculations (<12%) that are dwarfed by the standard deviation of mean VEIW. Moreover, variation in VEIW with distance from the pulp cavity likely reflects idiosyncratic patterns related to life history, which are difficult to control for; however, we recommend increasing raw VEIW data to minimize this effect. Our data reveal only a weak correlation between mean VEIW and body length, suggesting minimal ontogenetic impacts for the calculations of TFT and TRR. Finally, we provide a relative standard deviation of mean VEIW for *Alligator* of 29.94%, which can be

used by researchers to create data-driven error bars for TFTs and TRRs in fossil taxa with small sample sizes. We caution that small differences in mean VEIW calculations resulting from non-standardized sampling protocols, especially in a comparative context, will produce inflated error in TFT estimations that intensify with crown height. The same holds true for applications of our relative SD to TFT calculations in extinct taxa, which produce highly variable maximum and minimum TFT estimates in large-toothed taxa (e.g.,718–1331 days in *Tyrannosaurus*).

Sampling Impacts the Assessment of Tooth Growth and Replacement Rates in Archosaurs: Implications for Paleontological Studies

by
Jens Carl Dieter Kosch

A Thesis submitted to the Graduate Faculty of
North Carolina State University
in partial fulfillment of the
requirements for the degree of
Master of Science

Zoology

Raleigh, North Carolina
2020

APPROVED BY:

Lindsay Zanno Co-Chair of Advisory Committee	Mary Schweitzer Co-Chair of Advisory Committee
Adam Hartstone-Rose	Randall Langerhans
Michael D'Emic External Member	

DEDICATION

For my parents, who encouraged me to pursue my dream

For my teachers, who brought me closer to this dream, and sometimes stopped me from trying to run before I learned how to walk at a proper pace

And

For my friends and extended family, who reminded me that I am never truly alone

BIOGRAPHY

Jens became deeply interested in dinosaurs when he watched the 1955 Czechoslovakian movie Journey to the Beginning of Time on TV at the tender age of 3.5 years. His interest never diminished but expanded in the intellectually stimulating environment his family provided to include paleontology, (ancient-)history, biology, and geology. Yet he firmly kept becoming a paleontologist as his main goal in sight that pushed him trough school.

After acquiring his Bachelor's and Master's degree in geological sciences at the Freie Universität Berlin with the study of the dentigerous elements of *Dicraeosaurus* and *Giraffatitan* Jens continued to follow this fascinating path on the trail of the biggest terrestrial animals that ever lived, sauropods, and it took him to NC State University and the Zanno lab. There he enjoyed the opportunity to partake in fieldwork and one summer it provided him with the opportunity to travel to all East Coast museums with sizable sauropod collections by bus. As part of his research he worked on *Alligator* dentitions in order to elucidate tooth growth and sampling effects in the study of archosaur dentitions.

Jens plans to continue work in paleontology, preferably in Europe so he can be closer to his family and friends in the homeland while working on publications that exceed the scope of this Masters Thesis.

TABLE OF CONTENTS

LIST OF TABLES

LIST OF FIGURES

Sampling Impacts the Assessment of Tooth Growth and Replacement Rates in Archosaurs: Implications for Paleontological Studies

Abstract

Dietary habits in extinct species cannot be directly observed; thus, in the absence of extraordinary evidence, the dietary ecology of extinct species must be reconstructed with a combination of morphological proxies. Such proxies often include information on dental organization and function such as tooth formation time (TFT) and replacement rate (TRR). In extinct organisms, TFT and TRR are calculated, in part via extrapolation of the space between incremental lines in dental tissues representing daily growth (von Ebner Line Increment Width; VEIW). Tooth formation times and replacement rates in extinct species are becoming regularly calculated; however, to date, little work has been conducted testing assumptions about the primary data underpinning these calculations, specifically, the potential impact of differential sampling and data extrapolation protocols. To address this, we tested a variety of intradental, intramandibular, and ontogentic sampling effects on calculations of mean VEIW, TFT, and TRR using histological sections and CT reconstructions of a growth series of three specimens of the extant archosaurian *Alligator mississippiensis*.

We find transect position within the tooth and orientation with respect to VELs to have the greatest impact on calculations of mean VEIW—a maximum number of VEIW measurements should be made as near to the central axis as possible. Measuring in more crowded regions of the tooth off the central axis can reduce mean VEIW by 36%, causing inflated TFT calculations. We find little demonstrable impact to calculations of mean VEIW from the practice of subsampling along a transect, or from using mean VEIW derived from one portion of the dentition to extrapolate TFT and TRR for other regions of the dentition. Subsampling along transects contributes only minor variation in mean VEIW calculations (<12%) that are dwarfed by the standard deviation of mean VEIW. Moreover, variation in VEIW with distance from the pulp cavity likely reflects idiosyncratic patterns related to life history,

which are difficult to control for; however, we recommend increasing raw VEIW data to minimize this effect. Our data reveal only a weak correlation between mean VEIW and body length, suggesting minimal ontogenetic impacts for the calculations of TFT and TRR. Finally, we provide a relative standard deviation of mean VEIW for *Alligator* of 29.94%, which can be used by researchers to create data-driven error bars for TFTs and TRRs in fossil taxa with small sample sizes. We caution that small differences in mean VEIW calculations resulting from non-standardized sampling protocols, especially in a comparative context, will produce inflated error in TFT estimations that intensify with crown height. The same holds true for applications of our relative SD to TFT calculations in extinct taxa, which produce highly variable maximum and minimum TFT estimates in large-toothed taxa (e.g.,718–1331 days in *Tyrannosaurus*).

Introduction

Tooth replacement rate (**TRR**) provides key information on the function and evolution of the dentition (Edmund 1960, Osborn 1970, 1975, Richman et al. 2013, Whitlock and Richman 2013, Schwarz et al. 2015, LeBlanc et al. 2016, Bramble et al. 2017) that can be used to infer aspects of the paleobiology of extinct taxa such as metabolic activity/investment, dietary preferences and behavior (Johnston 1979, Barrett 2014, Salakka 2014, D'Emic et al. 2013, 2019a, 2019b, Brink et al. 2015, Button et al. 2017; D'Emic et al. 2019). However, tooth growth and exfoliation cannot be directly observed in extinct species, therefore TRR in extinct taxa must be estimated via growth lines preserved within dentin (von Ebner Lines, **VEL**s) and/or incremental growth lines of enamel that record different rhythms (see Smith 2004 for a review). Within living archosaurs, VELs are known to represent daily dentin deposition (Erickson 1992, 1996a). Paleontological studies have therefore used VEL count, or estimates of VEL count derived from direct measurements of dentin thickness divided by the mean width between VELs (so called "von Ebner Line Increment Width", **VEIW**), to estimate tooth formation times (**TFT**s) and TRR in extinct species (e.g., Erickson 1996b, Sereno et al. 2007, D'Emic et al. 2013, 2019b, Garcia and Zurriaguz 2016, Erickson et al. 2017, Ricart et al. 2019). This practice makes the accurate estimation of VEL counts and mean VEIW a critical consideration, as errors in the calculation of either will have cascading effects on estimations of TFT and TRRs, ultimately resulting in erroneous paleobiological inferences and macroevolutionary trends.

The challenges of working with fossil data constrain sampling approaches for deriving VEL count and mean VEIW in extinct species. For example, because a researcher cannot always choose the location or orientation for consumptive sampling, mean VEIWs are often calculated from, and then applied to, different transect locations within the same tooth (Erickson 1992, 1996b, Sereno et al. 2007, Gren 2011, D'Emic et al. 2013, 2019b Gren and Lindgren 2013, García and Zurriaguz 2016, Kear et al. 2017, Ricart et al. 2019) or calculated from, and then applied to, different tooth positions within the jaw (Kosch 2014, Schwarz et al. 2015, García and Zurriaguz 2016, D'Emic 2019a, 2019b). Moreover, because VELs are not always visible along the entire transect, mean VEIWs are typically derived from a transect subsample, as opposed to being calculated from the entire transect length (Erickson 1992, 1996a, 1996b, Gren 2011, Gren

and Lindgren 2013, Button et al. 2017, Erickson et al. 2017, Kear et al. 2017, Ricart et al. 2019, D'Emic et al. 2019b).

These practices rely on a series of data extrapolations that can introduce possible intradental and intramandibular sampling effects. Intradental data extrapolations are often based on one or multiple of the following assumptions: 1) mean VEIW is constant regardless of the developmental age of the tooth (i.e., does not vary significantly or consistently with distance from the pulp cavity); 2) the maximum number of VELs (used to derive TFT) are preserved at any transect location (i.e., a transect taken anywhere on the tooth from pulp cavity to crown will capture all VELs reflecting the maximum age of the tooth); and 3) mean VEIW is consistent regardless of the transect position used for sampling (i.e., does not vary across the tooth). Assumption 1 forms the basis for using a subsection of a transect to derive a mean VEIW for a tooth (Erickson 1992, 1996a, 1996b, Gren 2011, Gren and Lindgren 2013, Erickson et al. 2017, Kear et al. 2017, Ricart et al. 2019, D'Emic et al. 2019b), but contrasts with a competing hypothesis that teeth have different growth rates during their formation, which would result in wider VEIWs depending on distance from the pulp cavity (Yun-Hsin Wu personal communication, Lawson et al. 1971, Hanai and Tsuihiji 2018, Finger et al. 2019), as well as with observations of flexible replacement rates coupled with metabolic activity (often seasonally influenced) in extant reptiles (Cooper (1966) in *Anguis fragilis*, Delgado et al. (2003) in *Chalcides sexlineatus* and *Chalcides viridanus*)) and mammals (Klevezal 1996: 66f). Assumption 2 forms the basis for the use of transverse sections to derive TFTs (Sereno et al. 2007, Gren 2011, Gren and Lindgren 2013, Kear et al. 2017, Ricart et al. 2019). This assumption was criticized by D'Emic et al. (2013) on grounds that not all VELs present in a tooth are exposed in transverse section. Assumption 3 forms the basis for approaches that measure VEIWs and calculate a mean VEIW based on transects that stretch from the tooth's center near the pulp cavity to the marginal parts of the tooth, either in transverse sections of the tooth (Gren 2011, Gren and Lindgren 2013, Kear et al. 2017, Ricart et al. 2019) or multiple groups of measurements in a longitudinal section ("zig-zag pattern", Erickson 1992, 1996a, 1996b, D'Emic et al. 2013, 2019b [in part]).

Not only is it difficult to mitigate intradental sampling effects, one cannot generally sample all teeth in a mandible; therefore, many studies rely on the assumption that VEIW is

constant across the tooth row. For example, previous studies of fossil archosaurs utilizing VEL counts and/or mean VEIW to derive TFTs and TRRs, base these estimates on teeth within a single respective tooth family within the dentition (either mesial teeth [Erickson 1992, 1996a, Sereno et al. 2007, D'Emic et al. 2013], unspecified "mean-sized teeth" [Erickson 1996b, Erickson et al. 2017], molariform distal teeth [Ricart et al. 2019], or isolated teeth of uncertain position within the jaw [Garcia and Zurriaguz 2016, D'Emic 2019b]). The use of "mean sized teeth" (Erickson 1992, 1996a, 1996b) relies on the assumption that mean VEIW does not differ systematically according to tooth position and thus is constant in all tooth positions. D'Emic et al (2013) derived a mean VEIW from premaxillary teeth in sauropods; however, subsequent studies applied transfer functions for tooth length to whole dentitions to derive TFT in sauropods (Schwarz et al. 2015, Kosch 2014, D'Emic 2019a). In a similar fashion, D'Emic et al. (2019b) applied mean VEIW derived from isolated teeth from various mandibular elements of theropods to other mandibular elements to estimate TFT and TRR. In these instances, the assumption is that data derived from one tooth position can reliably be applied to a tooth from a different tooth position. This practice has the potential to introduce intramandibular sampling effects into calculations of TFT and TRR. Finally, Erickson (1992, 1996a, 1996b) concluded that VEIW changes during ontogeny, with wider VEIWs characterizing larger individuals. Such differences could introduce ontogenetic sampling effects into the derivation of TFT and TRR in extinct species.

Here we explore the impact of intradental, intramandibular, and ontogenetic sampling effects on calculations of mean VIEW, TFT, and TRR by sampling multiple teeth along the tooth row of different ontogenetic stages of the extant archosaurian taxon *Alligator mississippiensis*. We test the following hypotheses: 1) sampling transects taken in different orientations to VELs will not produce significantly different calculations of TFT; 2) measuring VEIWs at different distances from the pulp cavity along the central axis (**CA**) will not result in significantly different mean VEIWs; 3) sampling transects taken in different regions of the tooth (with regard to the tooth from root to apex) will not produce significantly different VEIWs and thus different TFTs; 4) sampling different tooth positions within the jaw will not produce different calculations of TFT; and 5) sampling during different growth stages will not result in different calculations of mean VEIW. We also explore the distribution of VEIW within our sample and apply standard

deviations derived from an extant archosaur to existing TFT data for extinct taxa, to assess the potential impact of VEIW calculation on TFT and TRR data in fossil vertebrates. The results serve to inform best practices for sampling in studies of dental organization and begin to quantify potential error in tooth growth and replacement rate estimates in extinct taxa.

Abbreviations

CA central axis, **CH** crown height, **CAH** central axis height, **DDR** dentin deposition rate, **Dent** dentary tooth position, **EDJ** enamel dentin junction, **FL** femur length, **FTS** formation time slope, **ML** mandible length, **Mx** maxillary tooth position, **Pmx** premaxillary tooth position, **SD** standard deviation, **TFT** Tooth Formation Time, **TH** tooth height, **TRR** Tooth Replacement Rate, **VEL** von Ebner Line, **VEIW** von Ebner Increment Width between von Ebner Lines

Methods

Specimens and Sampling

To assess ontogenetic sampling effects, we examined the dentition across an ontogenetic series of three individuals of *Alligator mississippiensis*. We estimated body length of our two smallest specimens using the regressions of Farlow et al. (2005) (femur length [**FL**] against body length). Our smallest individual (NCSM 100803) has an estimated body length of 37.1 cm (FL=24.55 mm), which corresponds to the size expected of young yearling (larger than a hatchling but 33% smaller than a yearling at the end of its first year) (Khan and Tansel 2000) (Fig. 1A,D,G) and our medium sized individual (NCSM 100804) has an estimated body length of 90.6 cm (FL=61.58), corresponding to the upper end of the size range expected of a two year old (Khan and Tansel 2000) (Fig. 1B, E, H). There was no associated femur with our largest specimen (NCSM 100805), therefore we used two methods to approximate an estimated body length range (Fig. 1C, F, I). We used mandible length (**ML**) as a proxy for skull length, which we then used to estimate total length from the regressions in Farlow et al. (2005). We also used ML to estimate Snout-Vent length, and then derive total body length using regression equations derived by Wu et al. (2006) for the congener *A. sinensis*. These produced an estimated body length of between 3.6 - 3.9 m, which corresponds to an age of more than sixteen years according

to Khan and Tansel (2000). No life history data was available for the specimens, the estimated ages correspond to the size range given for age categories in table 3 of Khan and Tansel (2000), following Neill (1971).

All material was scanned at Duke University in a micro-CT Nikon XTH 225 ST. CT images were taken with a setting of 170 kV and 86 mA and slice thickness of 31.7 µm for the small *Alligator* (NCSM 100803). The skull of the medium sized *Alligator* (NCSM 100804) was scanned in two scan processes, one with 135 kV and154 mA and one with 130 kV and 170 mA, both with a slice thickness of 45.2 µm. For the large *Alligator* (NCSM 100805) the upper and the lower jaw where both scanned in three scanning processes each with 150 kV and 134 to 139 mA for the upper jaw and 150 kV to 139 to 144 mA for the lower jaw and a slice thickness of 61.3 µm. All files were saved in .tif format. Data reconstruction was done with a RECO1 workstation. Composite files for the entire skulls (small [NCSM 100803] and medium [NCSM 100804] sized *Alligator*) or complete elements (upper jaw and lower jaw of the large *Alligator* [NCSM 100805]) were constructed in AVIZO 9.0. Those files were used for two different purposes: an initial inspection that aided in the decision which alveoli should be sampled for histological sections of teeth and surrounding tissue, and to create digital models of the teeth in order to ascertain measurements of functional and replacement teeth of the quadrant of the jaw from which histological samples would be taken. Foremost among these measurements was central axis height (**CAH**), the distance between the tip of the pulp cavity and the crown apex, which equals the sum of all VEIWs measured along the central axis (plus apical enamel thickness). The combination of resolution and contrast of the x-ray micro-CT scans does not allow for the clear distinction of the enamel dentin junction (**EDJ**) in all teeth (Jones et al. 2018).

We chose twelve tooth positions that exhibited both a functional tooth and replacement teeth for sampling (Pmx 1, Pmx3, Mx 6, Mx 7, Mx 12, Mx 13, Dent 2, Dent 4, Dent 11, Dent 12, Dent 18, Dent 19). The distalmost teeth of the largest specimen [NCSM 100805] were not preserved, therefore we approximated these tooth positions by sampling the 15th and 16th alveolus. Sampling of multiple tooth positions across the length of each dentary helped to access intramandibular sampling effects. Some of our data collection required sampling of the same position across multiple individuals. In these cases, we chose a subset of tooth positions that possessed at least one functional tooth and at least one replacement tooth (mesial dentition only

as distal dentition often lacked replacement teeth) and also represented a widespread distribution across the tooth row and dentigerous elements (mesial premaxillary teeth, mesial and distal maxillary teeth, and their counterparts in the dentary) across all three individuals.

Histology

Histological slides were prepared following standard thin-sectioning protocols (Lamm 2013). First, the respective areas of interest were separated using a diamond bladed ISOMET 1000 precision saw. The segments were prepared for embedding by dehydration in progressive ethanol baths (70%, 90%, 100%) and defatted in acetone. Samples were not demineralized, which is known to cause shrinkage (Dean 1998, Smith 2004) and can impact tooth measurements. Next, the samples were embedded in Epo-Tek 301 Epoxy Resin. No staining was performed. The embedded jaw elements were cut close to the intended plane of the section (Fig. 2) and ground using silica carbide paper (120–1200 grit) before being fixed to a slide, cut again and grind down to 0.13-0.56 mm thickness. The sections were studied with a Nikon Eclipse Ci POL microscope equipped with a polarizer and a lambda filter, and photographed using an iPhone 7 camera or a Rollei Powerflex 470 camera.

VEL Count and Measurements

Photographs were either stitched together into a composite within Adobe Photoshop 2015 or directly opened in Image J, whereupon a transect line was applied and the sections of the VEL crossing the transect were marked with an arrow symbol. Increment widths were measured using the Image J inbuilt measurement tool and measurements were exported to Excel 2015 to compute averages. Minimum and maximum VEIW in a given transect were used in combination with the transect length and the central axis height to compute absolute maximum and minimum tooth ages represented by the measured transect and the tooth respectively. Upper and lower limits of TFT were computed by subtracting (for maximum ages) and adding (for minimum ages) the standard deviation (**SD**) of the VEIW from the mean VEIW and applying these values to the transect length and the central axis height. This strategy of measuring VEIWs allowed us to test the assumptions that data derived from one tooth position can reliably be applied to a tooth from a different tooth position and that mean VEIW does not vary significantly or consistently with distance from the pulp cavity.

Hierarchically there are three different mean VEIWs used in different steps. The mean VEIW of a transect, as described above; the mean VEIW of all transects of a tooth, which was used in calculating the TFT used to determine TRR; the mean VEIW of a specimen was used to compare VEIW through ontogeny and with other datasets. TH and CAH were measured in AVIZO 9.0 (Fig. 1).

In the large *Alligator* [NCSM 100805] some tooth crowns were damaged, with small chips of the apices missing and cracks running through parts of the crown. Some also showed a considerable degree of tooth wear. In these cases, the crowns were digitally reconstructed to their full height in Avizo. Cracks and missing chips were digitally infilled with voxels assigned as reconstructed dentin up to a point where tooth wear was visible if signs of wear could be identified. Further reconstruction followed the curvature of the crown's shape, covering every exposed dentin surface with a layer at least two voxels deep that were assigned to a different material that represents dentin and enamel lost in tooth wear. These reconstructed crowns were used when measuring CAH and TH for these teeth. The original values without reconstruction are presented in the supplementary material (S3).

Our raw measurement of CAH and TH include both enamel and dentin thickness. The enamel layer in extant crocodylians is thin (Enax et al. 2013) and scales nearly isometrically (Schmiegelow et al. 2016, Sellers et al. 2019), with minor changes related to tooth shape (intrafamilial heterodonty) (Osborn 1975, Kieser et al. 1993, Gignac 2010, D'Amore et al. 2019) as opposed to size. To calculate CAH as a measure of dentin only, we subtracted the average enamel thickness value, and used this corrected CAH value in our calculations. The average enamel thickness was derived from measurements perpendicular to the EDJ taken from photographs of thin sections of representative teeth using the measurement tool in ImageJ. For the small [NCSM 100803] and medium [NCSM 100804] sized specimens three photographs with up to four measurements around the apical half of the crown in each photograph were used to calculate an average enamel thickness; for the large specimen [NCSM 100805] two photographs were used.

We could directly measure VEIW in all but two-sampled teeth (first Pmx and 11th Mx teeth in the small *Alligator* [NCSM 100803]); these teeth were not considered further. We

reconstructed TFT and TRR from mean VEIW taken from direct measurements of the remaining samples.

Transect Orientation

To determine the impact of sectioning strategy (intradental sampling effects) on calculation of VEL counts, and specifically to test the assumption that mean VEIW is consistent regardless of the transect position used for sampling, we counted VELs across transects taken at multiple angles from the 12th Mx, 12th Dent, and 18th Dent tooth of (NCSM 100804, medium-sized *Alligator*). Transect positions were categorized as base-apex (Fig. 3a; from the tip of the pulp cavity to the crow apex [this is equal to the full CAH]); near-crown-apex (Fig. 3b; measured at the tooth apex, yet not along the CA); mid-crown (Fig. 3c; measured in the central part of the crown); crown base (Fig. 3d; transect from the tip of the pulp cavity to EDJ almost perpendicular to the CA); root-base (Fig. 3e; measured from the pulp cavity near the root base to the lateral dentin border); mid-root (Fig. 3f; measured from the pulp cavity at the mid root to the lateral dentin border); root-apex (Fig. 3g; measured from the pulp cavity near the root tip to the lateral dentin border).

Hypotheses testing

1. We tested the hypothesis that sampling transects taken in different orientations to VELs will not produce significantly different calculations of TFT by comparing VEIWs from transects taken perpendicular and oblique to VELs. We present the difference in TFT in days and in percent differences, and performed a paired t-test of the TFTs to test for significance.

2. We tested the hypothesis that measuring VEIWs at different distances from the pulp cavity will not result in significantly different mean VEIWs by comparing mean VEIW and resulting TFT calculations derived from eight distinct subsamples along the same transect in Dent 11 of the large specimen [NCSM 100805] and mean VEIWs of three different sections along this transect. Subsamples were taken along the CA at different distances from the pulp cavity (one apical, one basal and six in various parts of the mid crown region). This approach attempts to capture variation in growth rate during the formation of a tooth using a CA transect only. An ANOVA was performed to test the significance of the differences between the means of

apical, basal and mid crown VEIWs and followed by a post-hoc Tukey-Kramer test comparing the VEIWs of the apical versus mid crown, apical versus basal, and mid crown versus. basal sections.

3. We tested the hypothesis that sampling transects taken in different regions of the tooth (with regard to the tooth from root to apex) will not produce significantly different VEIWs or different TFTs using multiple approaches.

We assessed the impact of calculating TFT from transects located at regions around the tooth other than the CA by calculating alternative TFTs using a mean VEIW and transect length from a region of the tooth off the central axis (CA) and dividing this by a TFT derived from a CA transect (= true TFT, where both mean VEIW and CAH were derived along the CA). A mean of these values was used to determine what percentage of the true TFT was captured by TFTs taken from transects not on the CA.

We also assessed the impact of subsampling along transects not located along the CA. For this, we calculated mean VEIW from subsamples of three transects closest and most distant from the CA and calculated TFTs using CAH derived from a CA transect. These mean VEIWs represent extreme end members for VEIW thickness primarily related to tooth geometry as opposed to growth that can be derived from subsampling different regions of the tooth other than the CA. We express the difference in the TFT estimates as a percent calculated by dividing the TFT based on the portion furthest from the CA by the TFT obtained from the portion closest to the CA. We test the significance of the difference between the VEIWs from close and most distant to the CA with a two-sample t-test assuming unequal variances.

Additionally, the change in resolution of VEL with increasing distance from the pulp cavity in lateral transects was tested in a theoretical framework by creating a figure (Fig. 3) with VELs in the same orientations and relative distances from each other and counting the number of VEL crossed by transects drawn in the tooth and the number of VEL visible under a magnification that mimics the resolution achieved under a microscope.

4. We tested the hypothesis that sampling VEIW at different tooth positions within the jaw will not produce different calculations of TFT in two ways.

First, the mean VEIWs for all sampled tooth positions obtained from transects with a similar orientation were subjected to an ANOVA to test if significant differences between their means exist. To test the amount of error a researcher could encounter if using the mean VEIW derived randomly from anywhere in the dentition to calculate the TFT of the remainder of the dentition, we calculated the grand mean standard deviation (SD) of the VEIW derived from all transects taken along the CA and applied this SD range of the VEIW to the VEIWs used to calculate TFTs. The grand mean SD is subtracted from the mean VEIW of the tooth to obtain a minimum VEIW and added to obtain a maximum VEIW. TFT is derived from dividing the CAH (from the tip of the pulp cavity to crown apex) by those VEIWs. The fit of the minimum and maximum mean VEIW based TFTs was compared to the TFTs of the sampled teeth by performing a two-sample t-test for unequal variances in MS Excel (Excel for Office 365 16.0.11328.20362). The difference between the TFT and the TFTs based on SD modified VEIWs is shown as TFT values in days, differences in TFT in days and percent differences of the minimum and maximum TFTs to the baseline TFTs.

5. We tested the hypothesis that sampling during different growth stages of an organism's life history will result in different calculations of mean VEIW by investigating the relationship between VEIW and body length and TRR and body length using ordinary least squares regression, utilizing the RSQ function to derive R^2 and the FDIST function to arrive at a significance p. For other plots the coefficient of determination (R^2) was determined using the inbuilt functionality of MS Excel (Excel for Office 365 16.0.11328.20362) for charts. Additionally, we performed an ANOVA on the same dataset created for testing hypothesis 4, but here grouped by ontogenetic stage. Using the specimens as groups we can make inferences about the presence or absence of differences in the mean VEIW during ontogeny.

Application to Fossil Taxa

We used the mean SD of *Alligator* to derive an estimated SD for the TFTs calculated for archosaurs in Erickson (1996b) and Garcia and Zurriaguz (2016) both of which reported VEIW ranges, but no SDs. We also used the reported SD for several theropods in D'Emic (2019b) as an opportunity to test the efficacy of applying the relative SD of *Alligator* to other archosaurs when not enough data on VEIW is available to confidently derive SD on the raw data. For this we

compared actual SD values calculated in D'Emic (control values) to SD estimates for those same taxa that we derived by applying the relative SD from *Alligator* (approximated values). To calculate approximated values, we derived a relative SD for *Alligator* by dividing mean VEIW by grand mean SD, and then divided reported VEIWs for archosaurs from D'Emic (2019b), Erickson (1996b), and Garcia and Zurriaguz (2016) by the relative SD of *Alligator*. Central axis height (from the tip of the pulp cavity to the crown apex) was derived by multiplying the reported mean VEIW with the reported TFT. The central axis height was then divided by the VEIW plus or minus SD to derive upper and lower ends to the range of possible tooth ages.

We also explore the effect of applying the relative SD of *Alligator* on calculations of TFT and TRR in sauropods using mean VEIW±1SD. We followed a similar approach using data from D'Emic et al. (2013, 2019a), Sattler (2014), Kosch (2014), Schwarz et al. (2015). For the sauropod data, we calculated the resulting minimum, maximum and baseline TFTs and the TRRs derived from them, and summarized these data as mean TFTs and TRRs, which are presented as summaries for each tooth position (functional, replacement tooth one, replacement tooth two, etc…). This representation of TFT and TRR is analogous to how these values are calculated in D'Emic et al. (2013, 2019b), Sattler (2014), Kosch (2014), and Schwarz et al. (2015). All originally reported TFTs in these publications are based on the transfer functions of tooth height to TFT of D'Emic et al. (2013), using the function for narrow crowned taxa derived from sampling *Diplodocus* Pmx teeth for *Dicraeosaurus* and *Tornieria* and the function for broad crowned taxa derived from *Camarasaurus* Pmx teeth for *Giraffatitan* and *Brachiosaurus*. For all teeth, a mean VEIW of 15 μm was assumed, derived from D'Emic et al.'s (2013) calculation of mean VEIW for both *Dipldocus* and *Camarasaurus*.

As reported, TRRs represent a mean value derived from all TRRs that could be obtained (and might differ slightly from TRRs that are calculated subtracting the mean TFTs of those positions from one another due to empty tooth positions in some tooth families). TRR max-max is derived using VEIW-1SD to calculate maximal TFT for both teeth in a tooth family. TRR min-min is derived using VEIW+1SD to calculate minimal TFT for both teeth in a tooth family. TRR min-max and TRR max-min are derived by subtracting TFTs calculated using VEIW+1SD and VEIW-1SD. TRR min-max applies VEIW+1SD to calculate minimum TFT for the oldest tooth in a successional pair of teeth in a tooth family and VEIW-1SD for the youngest tooth in

the pair, whereas TRR max-min, takes the opposite approach. We obtained the mean TFT and mean values from TRRs for each tooth position for the completely sampled dentitions of *Tornieria*, *Giraffatitan* and *Dicraeosaurus.* Whereas for the more sporadically sampled dentitions of *Camarasaurus* (UMNH 5527) and *Diplodocus* (YPM 4677) and *Brachiosaurus* (USNM 5730) we present the range of reported TFTs for each position in the Pmx or Mx and Dent. We also compare the reported SD for the theropods *Majungasaurus*, *Ceratosaurus*, and *Allosaurus* from D'Emic et al. (2019b) directly with the SD derived from applying the relative SD based on the *Alligator* sample to the mean VEIWs of these theropods.

Results

The potential emergence of intradental sampling effects is focused on aspects of transect orientation, transect position, and sampling distance from the pulp cavity (VEIW variation during the formation of a tooth). Potential intramandibular sampling effects and ontogenetic sampling effects are addressed as aspects of tooth position and specimen age, respectively.

Intradental effects:

Hypothesis 1: Sampling transects taken in different orientations to VELs (perpendicular or obliquely oriented to VELs) (Fig 2, 3, 4) will not produce significantly different calculations of TFT.

Transect orientation is important for precise estimates of mean VEIW and TFT/TRR. Transects that cross VELs obliquely (Fig. 4, Fig. S1, 3) (e.g., top of the pulp cavity to the EDJ, in areas adjacent to the apex (Fig. 3b) yield VEIWs up to twice the width as those made perpendicular to VEL trendlines. This, of course, aligns with basic geometric principles and can be used to reject this hypothesis if the different mean VEIWs derived from perpendicular and oblique transects are then applied to the same transect length (e.g. CAH) to derive TFT. Table 1 illustrates these differences with 33% to 20% shorter TFTs calculated when mean VEIW is derived from obliquely oriented measurements compared to those based on perpendicularly oriented measurements when crown height is derived from the CAH for three pairs of oblique and perpendicular series of measurements and the TFT based on them. This is a significant difference, paired t-test, $t_2 = 10.36$ [$t_{crit} = 4.30$] $p < 0.05$ [0.009], mean difference 64 days. However, if a researcher were to use the *same* transect to derive mean VEIW and transect length

in calculations of TFT the effect is less. Oblique transects result in both a larger mean VEIW and a longer transect, whereas perpendicular transects are composed of shorter VEIWs across a shorter transect. Nevertheless, both approaches underestimate age compared to transects along the true CA because they fail to account for the apical-most component in derivations of CAH (Fig. 2) (see hypothesis 3 below). In short, with regard to best practices in deriving TFT, that is to say, always using CAH for transect length, we can reject the hypothesis that measuring oblique to VEL orientation will not significantly affect TFT calculations.

Hypothesis 2: Measuring VEIWs at different distances from the pulp cavity along the CA will not result in significantly different calculations of mean VEIW.

We do not find a consistent trend of increasing or decreasing VEIW toward the crown base in our sampled teeth, yet note that in our sample, mean VEIWs for transects are narrowest when measured farthest from the pulp cavity. It is not clear if this is a common pattern across the tooth row as more teeth would need to be sampled. We find that measuring the VEIWs at different distances from the pulp cavity along the CA yields a calculated mean VEIW that varies by 11-12% (Fig. 5). In case of the eight transects sampled presented in Fig. 5 an ANOVA between the 86 VEIWs measured for the crown apex, the 348 VEIWs of the combined six mid crown transects, and the 42 VEIWs of the crown base finds significant differences between the VEIWs in the three regions of the tooth, $F_{2, 473} = 7.52$ [$F_{crit} = 2.62$], $p < 0.05$ [0.0006]. However, the post-hoc Tukey-Kramer test of the VEIWs of the regions only finds significant difference between the VEIWs of the apical transect and the six mid-crown transects, $q_{432} = 5.449$ [$q_{crit} = 3.325$] $p < 0.05$ [0.000396] and between the apical VEIWs vs. basal VEIWs, $q_{126} = 3.336$ [$q_{crit} = 3.325$] $p < 0.05$ [0.04903]. We find no significant difference between mid crown VEIWs and basal VEIWs $q_{388} = 0.172$ [$q_{crit} = 3.325$] $p > 0.05$ [0.992].

Hypothesis 3: Sampling transects taken in different regions of the tooth (with regard to the tooth from root tip to apex) will not produce significantly different VEIWs.

We find transect position critical for precise estimates of mean VEIW and TFT and therefore our data refute this hypothesis, contradicting the assumption that mean VEIW is consistent regardless of the transect position used for sampling. With regard to location on the tooth, we find that sections that do not precisely section the CA do not preserve all VELs.

Transverse sections omit VELs, particularly those of the crown apex (Fig. 2). VEL counts along mesiodistal or labiolingual transects (lateral to the pulp cavity) are consistently fewer than those derived from a CA transect. This combined with the lack of resolution of VEL further from the pulp cavity results in much shorter calculated TFTs (TFTs calculated with this approach are only 83% on average of the TFT derived from a CA transect in NCSM 100804). We also find that mean VEIW in a tooth decreases laterally (Fig. 2, 3, Figs S1, 1, S1, 2) when sampled perpendicular to VEL trendlines; VEIWs are thickest along the CA from above the pulp cavity to the crown apex and thinnest near the EDJ in a transversal plane. The differences between these two groups are significant, $t_{80} = 5.40$ [$t_{Crit} = 1.99$], $p < 0.05$ [6.61451E-07]. Table 2 exemplifies this difference in VEIW thickness and resulting estimates if TFT is derived from VEIWs obtained from subsections of lateral transects other than the CA are then applied to CAH, particularly a subsample farthest from the CA. VEIW can be incorrectly measured by up to 36%, which would lead to inaccurately calculated TFT and TRRs.

Intramandibular effects:

Hypothesis 4: sampling different tooth positions within the jaw will not produce significantly different calculations of TFT.

Despite considerable variation in our calculations of VEIW values (ranging 5µm to 39µm within the sample and 6µm to 38µm within a single tooth), we find no statistical difference between mean VEIWs of tooth positions calculated across the tooth row (Table 3, Fig. 6), one-way ANOVA, $F_{10, 19} = 1.04$ [$F_{crit} = 2.38$], $p > 0.05$ [0.448]. If only the alveoli with three or more samples for an alveolus position (4 in alveolus 4, 6 in alveolus 11, 5 in alveolus 5, 4 in alveolus 18) are taken into account there is even less of a difference recovered, one-way ANOVA, $F_{3, 15} = 0.48$ [$F_{crit} = 3.29$], $p > 0.05$ [0.698]. The lack of systematic variation of VEIW in different teeth of mandibular quadrants and between lower and upper mandibles supports the assumptions that data derived from one tooth position can reliably be applied to a tooth from a different tooth position, supporting this hypothesis.

The (grand mean) SD of all VEIW measurements along the CA is 0.00479 mm, which is 29.94% of the mean VEIW of 0.0160 mm. Table 4 shows TFTs and TFTs calculated from mean VEIW ±1SD and Fig. 7 depicts the percent differences graphically. On average TFTs calculated

from mean VEIW -1SD are 48.78% bigger than the TFT and TFTs calculated from mean VEIW +1SD are 23.94% smaller. When tooth specific SDs are used these values change to 41.23% and 20.62% respectively (see table S2 and Fig. S2).

Two-sample, one sided t-tests between the unmodified TFTs and TFT calculated from mean VEIW ±1SD assuming unequal variances find a significant difference between TFT calculated from mean VEIW -1SD and the unmodified TFT ($p = 0.041$) but no significant difference for TFT calculated from mean VEIW +1SD (table 4). Whereas, no significant differences were found when using the tooth specific SDs instead of a grand mean SD (table S2).

As would be expected, the smaller the mean VEIW and the longer the CAH of the teeth under study, the more pronounced the influence the static grand mean SD has on derived TFTs. It is the size of the tooth that makes the TFT differences of maximum and minimum ages more or less pronounced on an absolute scale, not the position within the jaw.

Ontogenetic effects:

Hypothesis 5: sampling during different growth stages of an organism's life history will result in different calculations of mean VEIW.

When we derive mean VEIW for individual teeth with the same transect orientation and location and compare them among the sampled individuals (Fig. 6, table 3), we do not observe significant differences between individuals (one-way ANOVA, $F_{2, 35} = 2.29$ [$F_{crit} = 3.27$], $p > 0.05$ [0.116]). This indicates that specimen level mean VEIWs obtained by taking a mean VEIW from multiple teeth can be applied to teeth of individuals with a different ontogenetic status without producing significantly different results. When we derive mean VEIW across the whole dentition of just our sampled individuals (from smallest to largest: NCSM 100803, NCSM 100804, and NCSM 100805), we find a slight increase during ontogeny (Fig. S1, 5a); however, three individuals are not enough for a meaningful statistical comparison. When we add the mean VEIW of differently sized *Alligator* specimens ranging in body length from 0.60 m to 3.20 m derived from Erickson (1992 and 1996a), we find the relationship between VEIW and body length shows a weak ontogenetic signal ($R^2 = 0.389$) that still does not reach the level of 95% significance ($p = 0.074$) in an OLS regression (Fig. 8, Fig. S1, 5b).

Application to Fossil Taxa:

Table 5 gives the error margins for TFTs of various archosaurs included in the studies of Erickson et al. (1996b), Garcia and Zurriaguz (2016), and D'Emic et al. (2019b). Garcia and Zurriaguz (2016) only reported highest and lowest mean VEIWs and highest and lowest TFTs from their five-tooth sample, but never made clear if those values are directly related, pairing the lowest mean VEIW with the highest TFT, and they provided no measurements for the five teeth they sampled. We assume in table 5 that the highest age corresponds to the smallest VEIW and vice versa. The VEIW in these publications likely underestimate the VEIW as it would be measured along the CA, because Erickson (1996b), Garcia and Zurriaguz (2016), and in in part D'Emic et al. (2019b) based their calculations of VEIW on a combination of transverse sections and/or multiple measurements along transects perpendicular or semi-perpendicular to the CA and the VELs (see Fig. S1, 1b). We did not include the fossil crocodylians with reported VEIWs and TFTs from Ricart et al. (2019) in the table because they based their TFT calculations on the radius of dentine in their transverse sections instead of the central axis height, which means they are not representative of actual TFTs, whereas the TFTs reported by Erickson are supported by VEL counts for all regions where they were possible. As is to be expected, the greater the central axis height, the greater the variation in TFT produced by using mean VEIW±1SD. In an adult *Tyrannosaurus* with more than 15 mm central axis height (from the tip of the pulp cavity to the crown apex) the difference between minimum and maximum estimates of TFT is greater than a year and a half (613 days). Whereas, in the much shorter titanosaur tooth in our sample this difference is little more than five weeks (36 days).

D'Emic et al. (2019b) report SD for VEIW measurements of *Majungasaurus*, *Ceratosaurus*, and *Allosaurus*. One SD for *Majungasaurus* is 5.15µm (based on 54 mean VEIWs). We derive an approximated SD for *Majungasaurus* based on the relative SD of *Alligator* of 5.25µm, which compares closely to the control data (within 2%). For *Ceratosaurus*, we approximate a SD of 4.33µm, which is 33% greater than the actual SD of *Ceratosaurus* given in D'Emic et al. (2019b) of 3.26µm (based on the SD of 9 mean VEIWs). In *Allosaurus* the *Alligator* derived modified SD of 6.89µm greatly exceeds the SD (0.82µm) from the 4 mean VEIWs obtained by D'Emic et al. (2019b) by over 840%.

We also explore the effect of applying the relative SD of Alligator on calculations of TFT and TRR in sauropods (Table 6) using mean VEIW±1SD. Even with the range of TRR min-min and TRR max-max generated by using VEIW±1SD the TRR values for narrow crowned taxa (*Diplodocus*, *Torneria*, *Dicraeosaurus*) and broad crowned taxa (*Camarasaurus*, *Brachiosaurus*, *Giraffatitan*) do barely overlap, with the exception of the younger generation teeth [r3 or younger] of *Dicraeosaurus*, which are calculated to have longer replacement rates than younger teeth of their tooth families. TFTs based on VEIW±1SD between broad and narrow crowned taxa have more overlap. In all cases except for the distalmost tooth position in *Dicraeosaurus*, we derive a negative number for a mean TRR using TRR min-max (VEIW +1SD to calculate minimum TFT for the oldest tooth in a successional pair of teeth in a tooth family and VEIW -1SD for the youngest tooth in the pair), indicating that the "younger" replacement tooth [r2] would have formed before the "older" replacement tooth [r1], which is not biologically feasible. We caution against seeing this as a failure of using TFTs based on mean VEIWs to derive TRRs. It is rather unlikely that all VEIWs in a tooth will be at the upper end of the VEIW range and all in the preceding tooth in the lower range of VEIWs, especially if both teeth are still growing replacement teeth subjected to the same environmental factors affecting the organism forming parts both teeth at the same time.

Discussion

Currently our data do not support a straightforward trend in VEIW variation that can be linked to tooth growth over time. Within our sample, significant differences in mean VEIW occur between the apicalmost and thus oldest subsection of the tooth CA and sections grown later and thus it is tempting to suggest that subsampling VEIW either in the apicalmost or basalmost region of the tooth will lead to over or underestimates of TFT respectively. However, our sample contains a few replacement teeth (equivalents to the oldest and most apical crown parts of more mature teeth) that have wider mean VEIWs than the functional teeth in their respective alveoli (Table 6), which is at odds with the pattern we document of thinner VEIWs in the apical area. Moreover, when we compare multiple teeth of the same individual, we observe consistent patterns in VEIW that suggest external factors are influencing VEIW similarly within all teeth of the dentition. These conflicting data, suggest the crowded VELs we observe in our

sample is not reflective of a general pattern related to tooth growth that is consistent across individuals, but rather is likely related to individual variation in growth and ecology of the individual we sampled as VEIW variations along the CA likely represent life history data. Such an interpretation fits with other studies documenting variations in metabolic activity to TFT and TRR and thus daily tooth growth documented by VEIW across a wide array of tetrapods including squamates (*Anguis fragilis*, *Chalcides sexlineatus,* and *Chalcides viridanus*) (Cooper, 1966; Delgado et al., 2003) and mammals (Klevezal 1996: 66f). Future research into the underlying factors of tooth growth under controlled conditions (Wu et al. 2013) might provide more conclusive explanations for actual intradental VEIW variation. Thus, we caution that researchers should not interpret the pattern we document here of more crowded VELs early in tooth growth as applicable widely to *Alligator* or transferable to other archosaurs. What the data on subsampling do suggest is that subsampling VEIW anywhere along the central axis of the crown, as opposed to measuring VEIW along the entire CA can impact TFT calculation by up to 12%.

Variation in VEIW observed and VELs evident along transects off the central axis is more a function of tooth geometry than tooth growth and can have more extreme effects on calculations of TFT and TRR. We document that TFTs derived from mean VEIW of all VELs along transects lateral to the pulp cavity only capture about 83% of the age represented by the VEL along the CAH in part due to VEL that are represented along such transects but also because VEIW decreases in lateral transects by more than a third due to tooth shape. Measuring VEIW as close to the CA as possible mitigates problems introduced by other transect orientations and should be preferred over other methods such as measuring VEIWs in multiple transverse sections of the same tooth (Erickson 1992), particularly in high-crowned taxa. Mean VEIWs obtained by multiple transverse sections or a zig-zag pattern (S1, Fig. 1b) systematically underestimate the mean VEIW by conflating VEIWs of varying distance lateral of the pulp cavity, however, they are to be favored compared to transects that introduce error by measuring VEIW oblique to the VELs. Future research can make attempts to expand the dataset for crocodylians to include species with varying tooth geometry, including globidont taxa to see how tooth shape impacts VEIW and if different potential error margins have to be used when utilizing

VEIW measurements in teeth with morphology distinct from our *Alligator mississippienisis* sample.

Investigating ontogenetic sampling effects on mean VEIW is hampered by the small sample size of this study, but the ontogenetic development of dental organization we find differs from previously reported patterns (Edmund 1962, Erickson 1992, Hanai and Tsuihiji 2018). Erickson (1992) found a significant relationship between mean VEIW and body length in *Alligator*; however, we find no such strong evidence for ontogenetic sampling effects on mean VEIW. When we combine our data with that of Erickson's (1992 and 1996a) data, the relationship between mean VEIW and body length does not reach a level of 95% of significance. However, we note that a caveat of using the specimen level mean VEIWs from Erickson (1992 and 1996a) is that his VEIWs were derived from a "zig-zag" pattern of measurement (Fig. S1, 1b) (i.e., reported mean VEIWs combine VEIWs from near the CA and marginal measurements). Our data indicate that this technique leads to a systematic underestimation of VEIW compared to our CA-based measurements. Preliminary corrections for reported VEIWs of Erickson (1992, 1996a) by adding 26.667% to the reported width (following the assumption that 1/5 of the transects used by Erickson are using VEIWs that are 33% too short) do increase the correlation of body length to specimen mean VEIW to a significant value (OLS regression $p < 0.05$ [$p = 0.0455$], $R^2 = 0.457$; $R^2 = 0.680$ for a quadratic regression) (S1, Fig. 6, table 1). However, we do not deem this ad hoc correction of Erickson's (1992, 1996a) mean VEIWs precise enough to confidently apply it to all of his measurements obtained from Erickson's zig-zag counting and measuring method (e.g., in table 5). It is unclear if the addition of more data or a more reliable method to account for the systematically underestimated mean VEIWs of Erickson (1992, 1996a), will exacerbate the lack of correlation, or will more conclusively link mean VEIW and ontogenetic status. The former is consistent with the mostly small and non-systematic variation in mean VEIW of hadrosaur and theropod dinosaur species of different ontogenetic status reported in Erickson (1996b) and the constant VEIW in a juvenile and adult baurusuchid crocodylian reported by Ricard et al. (2019). As of now, our data cannot confidently support a simple trend of increasing VEIW during ontogeny that is strong enough to produce significant differences (α= 93% or more) in the mean VEIWs of our sampled teeth, but do suggest a slight ontogenetic increase in specimen mean VEIW. Due to the lack of significance of both of our

statistical tests our preliminary assessment is that VEIW does not change systematically and uniformly during ontogeny, making it possible to apply mean VEIWs obtained to various ontogenetic stages of a species without introducing an ontogenetic scaling factor.

Comparisons between broader taxonomic samples could be particularly problematic if the approach to measuring mean VEIW is not standardized. Based on our sampling tests, we propose the following best practices for calculating tooth ages.

1) If possible, obtain data on VEIWs from synchrotron scanning or histological sectioning (this approach is preferred over estimates of VEIW obtained from a transfer function).

2) Measure CAH from the tip of the pulp cavity to the crown apex for each tooth in the dentition via models obtained from CT scanning prior to preparation of histological sections. This approach is preferable as it is difficult to obtain a section from exactly the plane that contains both the crown apex and the tip of the pulp cavity.

3) Produce histological sections along the CA perpendicular to VELs. Teeth are three-dimensional objects. Deriving a histological section that precisely sections all VELs perpendicularly, even along the CA is practically impossible, a problem that is exacerbated by the fact that the CA follows tooth geometry and can be curved in some teeth. The effect of not producing an exact CA section perpendicular to all VELs mirrors the effect we document of measuring transects that are not perpendicular to the VEL, but would be expected to be much less severe in impact. The best method for approximating a precise CA section is to cut with the saw near the intended final plane of section and constantly monitor the final plane's orientation during grinding and polishing.

4) Measure the VEIW between all visible VEIW along the CA, avoiding subsampling. This protocol presents a practicality challenge as VEL in this region have the least optical contrast (Ricart et al. 2019, this study, personal communication Michael D'Emic) and are not always visible. If measuring VEL along the CA is not possible and transects must be taken in an alternate location, VEIW should be calculated perpendicular to VEL orientation as near to the CA as possible, and CAH measured along the true CA used to calculate TFT. Precise measurement of the CAH is important as it influences calculation of TFTs and TRRs.

5) Standard deviation (SD) from the average VEIW should be used to incorporate uncertainty into estimates.

The standard deviation of VEIWs found in our *Alligator* sample can be applied to mean VEIW in studies that don't include the standard deviation of their measured VEIWs or for taxa from which large datasets of VEIW cannot be directly measured. Comparisons of the SDs calculated from mean VEIWs of individual transects from D'Emic et al. (2019b) to SDs that result from applying the relative SD range of *Alligator* to other archosaurs indicates increasing similarity of the relative SD with increasing sample size, suggesting convergence on a confident measure of error that is widely applicable to archosaur datasets.

Although we find extreme differences in calculations of relative SD between our study on *Alligator* and taxa included in D'Emic et al. (2019b), we note that the difference these relative SDs is inversely related to the difference in the amount of underlying data used to generate SDs for each taxon. In other words, our relative SD (derived from the mean SD values of 87 individual transects with 4654 VEIWs) most closely approximates relative SDs of *Majungasaurus* from D'Emic et al. 2019b (which was based on 54 transects with 544 VEIWs), and differs most from the relative SD of *Allosaurus*, which was calculated using only 4 transects with 12 VEIWs (D'Emic et al. 2019b).

Thus, we find congruence of relative SD among large datasets of VEIW and suggest that applying the relative SD of *Alligator* we provide herein is a better approach for generating confidence intervals around mean VEIW for taxa in which a limited number of VEIW can be directly measured, as opposed to calculating SD from such a small number of measured VEIW. In addition, the *Alligator* based relative SD can be applied to TFTs calculated based on a transfer function like the transfer functions for tooth length to TFT form D'Emic et al. (2013, 2019b), which by their very nature cannot provide their own VEIW and VEIW SD and are thus based on the mean VEIW of the samples the transfer function was derived from. We advise to take values of minimum TFTs (from the mean VEIW + SD) and maximum TFTs (from the mean VEIW - SD) into account when calculating and discussing TRRs by comparing the TRRs based on minimum and maximum TFT values for both adjacent tooth positions to the calculated baseline value. These values are 42.73% older for maximum TFTs and -23.04% for minimum TFTs. This introduces a margin of error to reports of TFT and TRR.

6) In homodont to weakly heterodont taxa, researchers can be confident in applying mean VEIWs derived from transects perpendicular to VELs to derive calculations of TFT and TRR in other regions of the mandibles, and despite growth stage.

Conclusions

Our results indicate that the greatest challenges to accurately estimating TFT and calculating TRR for extinct taxa rests in 1) generating a transect perpendicular to VEL orientation for the measurement of VEIW (oblique measurements reduce TFT estimates by up to a third in *Alligator*); and 2) measuring VEIW and crown height along a transect that bisects the central axis as opposed to other regions of the tooth. VEIW decreases with increasing distance from the central axis (up to 36%) and use of mean VEIW values from these regions will produce inflated TFTs; the greater the crown height, the more intense the impact of using mean VEIW calculations from regions with more compressed VEL. Measuring VEIW along the central axis also helps to keep transect orientation perpendicular to VELs.

We find that transects misaligned with VEL orientation or with respect to the central axis impact the calculation of mean VEIW far more than the act of subsampling within transects, applying mean VEIW from one tooth in the mandible to crown axis height of another tooth, and ontogenetic status of the individual sampled. We document up to 12% variation in calculations of mean VEIW when derived from subsampling the CA transect and note that variation in VEIW is likely an idiosyncratic pattern linked to organismal life history. Therefore, we cannot recommend any standardized subsampling location along the central axis to approximate the mean and recommend directly measuring the distance between all visible VEL along the central axis to minimize error. However, we note that subsampling error is within the margin of error of VEIW ± 1 SD derived and therefore if a VEIW cannot be measured from a complete transect it is sufficient to use a subset of measurements along a CA transect to calculate a mean VEIW for a whole tooth. Intramandibular sampling effects do not significantly influence the mean VEIW as there is no systematic variation of mean VEIW associated with tooth position in the mandible in our sample. It is sufficient to have a few samples from teeth of a dentition to make reliable prediction of the TFT for other teeth, provided that the central axis height is known.

According to our limited data, ontogenetic status does not significantly affect calculations of mean VEIW (below a confidence value of $\alpha = 93\%$); therefore, we preliminarily suggest that a

mean VEIW obtained for a specimen of a taxon can be applied to the dentition of other specimens regardless of growth stage. However, we note that this factor warrants more study following the sampling protocols outlined in this study as ad hoc corrections of data for younger specimens of Alligator suggests the relationships might reach a higher degree of significance.

We provide a standard deviation (SD) for mean VEIW for Alligator of 29.94%, which is is consistent with recently published SD for theropod dinosaurs with large sample sizes (D'Emic et al., 2019b) and can be applied to VEIWs of other archosaurs without reported SDs or smaller sample sizes and thus help in creating realistic error bars for TFTs and TRRs. These confidence intervals are extreme in large-toothed taxa and call into question the reliability of TFT estimates that are based on few directly measured VEIWs as opposed to large raw datasets.

Our results add confidence to an intensifying body of research that uses approximations of tooth replacement rates and tooth formation times within the dentition of extinct vertebrates to derive paleobiological and evolutionary inferences, with the caveat that the primary data is consistent with the sampling approach we outline here. Future investigations into taxa with extreme heterodonty in somatically mature individuals and/or throughout ontogeny will add to our growing body of knowledge on best practices for investigating tooth growth and dental evolution in extinct vertebrates and may reveal nuanced sampling effects undetected in our study.

Acknowledgments

We thank Aurore Canoville for help with histological sections and training. Kristin Brink and Yun-Hsin Wu for discussions about dental organization and tooth replacement in *Alligator*. Appalachian State University for donations of Alligator specimens for consumptive sampling. Adam Hartstone-Rose and Edwin Dickinson for discussions on data interpretation and assistance with statistics. Mary Schweitzer, Brian Langerhans, Michael D'Emic, Christian Kammerer, and the staff and students of the Paleontology Research Lab at the NC Museum of Natural Sciences, for helpful critiques during project development.

References

Barrett PM. 2014. Paleobiology of Herbivorous Dinosaurs. Annual Review of Earth and Planetary Sciences 42: 207-230

Bramble K, LeBlanc ARH, Lamoureux DO, Wosik M, Currie PJ. 2017. Histological evidence for a dynamic dental battery in hadrosaurid dinosaurs. Scientific Reports 7: 15787 Doi:10.1038/s41598-017-16056-3

Brink KS, Reisz RR, LeBlanc ARH, Chang RS, Lee YC, Chiang CC, Huang T, Evans DC. 2015. Developmental and evolutionary novelty in the serrated teeth of theropod dinosaurs. Scientific Reports 2015; 5: 12338 https://doi.org/10.1038/srep12338 PMID: 26216577

Button K, You H, Kirkland JI, Zanno L. 2017. Incremental growth of therizinosaurian dental tissues: implications for dietary transitions in Theropoda. PeerJ 5:e4129; Doi 10.7717/peerj.4129

Cooper JS. 1966. Tooth replacement in the slow worm (*Anguis fragilis*). Journal of Zoology 150: 235–248.

D'Amore DC, Harmon M, Drumheller SK, Testin JJ. 2019. Quantitative heterodonty in Crocodylia: assessing size and shape across modern and extinct taxa. PeerJ 7:e6485 http://doi.org/10.7717/peerj.6485

D'Emic MD, Carrano MT. 2019a. Redescription of Brachiosaurid Sauropod Dinosaur Material From the Upper Jurassic Morrison Formation, Colorado, USA. The Anatomical Record DOI: 10.1002/ar.24198

D'Emic MD, O'Connor PM, Pascucci TR, Gavras JN, Mardakhayava E, Lund EK. 2019b. Evolution of high tooth replacement rates in theropod dinosaurs. PLoS ONE 14(11): e0224734. https://doi.org/10.1371/journal.pone.0224734

D'Emic MD, Whitlock JA, Smith KM, Fisher DC, Wilson JA. 2013. Evolution of High Tooth Replacement Rates in Sauropod Dinosaurs. PLoS ONE 8 (Issue 7): e69235. Doi:10.1371/journal.pone.0069235

Dean MC. 1998. Comparative observations on the spacing of short-period (von Ebner's) lines in dentine. Archives of Oral Biology 43: 1009-1021

Delgado S., Davit-Beal T, Sire J-Y. 2003. Dentition and Tooth Replacement Pattern in *Chalcides* (Squamata; Scincidae). Journal of Morphology 256: 146–159

Edmund AG 1960. Tooth replacement phenomena in lower vertebrates. Royal Ontario Museum Life Science Division Contribution 52: 1-190

Edmund AG. 1962. Sequence and Rate of Tooth Replacement in the Crocodilia. Royal Ontario Museum Life Sciences Division Contribution 56: 1-42

Enax J, Fabritius H-O, Rack A, Prymak O, Raabe D, Epple M. 2013. Characterization of crocodile teeth: Correlation of composition, microstructure, and hardness. Journal of Structural Biology 184: 155–163

Erickson GM. 1992. Verification of von Ebner incremental lines in extant and fossil archosaur dentine and tooth replacement rate assessment using counts of von Ebner lines. Master's Thesis Montana State University Bozeman, Montana, USA.

Erickson GM. 1996a. Daily deposition of dentine in juvenile *Alligator* and assessment of tooth replacement rates using incremental line counts. Journal of Morphology 228:189–194

Erickson GM. 1996b. Incremental lines of von Ebner in dinosaurs and the assessment of tooth replacement rates using growth line counts. Proceedings of the National Academy of Sciences of the United States of America 93:14623–7

Erickson GM, Zelenitsky DK, Kay DI, Norell MA. 2017. Dinosaur incubation periods directly determined from growth-line counts in embryonic teeth show reptilian-grade development. Proceedings of the National Academy of Sciences of the United States of America 114(3): 540-545

Farlow JO, Hurlburt GR, Elsey RM, Britton ARC, Langston W. 2005. Femoral Dimensions and Body Size of *Alligator mississippiensis*: Estimating the Size of Extinct Mesoeucrocodylians. Journal of Vertebrate Paleontology 25(2): 354–369

Finger JW Jr., Thomson PC, Isberg SR. 2019. A pilot study to understand tooth replacement in near-harvest farmed saltwater crocodiles (*Crocodylus porosus*): Implications for blemish induction. Aquaculture 504: 102–106

Garcia RA, Zurriaguz V. 2016. Histology of teeth and tooth attachment in titanosaurs (Dinosauria; Sauropoda). Cretaceous Research 57: 248e256

Gignac PM. 2010. Biomechanics and the Ontogeny of Feeding in the American Alligator (Alligator Mississippiensis [sic!]): Reconciling Factors Contributing to Intraspecific Niche Differentiation in a Large Bodied Vertebrate. Dissertation at Florida State University.

Gren JA. 2011. Dental histology of Cretaceous mosasaurs (Reptilia, Squamata): incremental growth lines in dentine and implications for tooth replacement. Examensarbeten i geologi vid Lunds universitet, Nr. 288, 18 pp. 45 hskp (45 ECTS credits) [Master's Thesis at Department of Earth and Ecosystem Sciences Division of Geology Lund University]

Gren, JA, Lindgren J. 2013. Dental histology of mosasaurs and a marine crocodylian from the Campanian (Upper Cretaceous) of southern Sweden: incremental growth lines and dentine formation rates. Geological Magazine, 151: 134–143

Hanai T, Tsuihiji T. 2018. Description of Tooth Ontogeny and Replacement Patterns in a Juvenile *Tarbosaurus baatar* (Dinosauria: Theropoda) Using CT-Scan Data. The Anatomical Record doi:10.1002/ar.24014

Jones MEH, Lucas PW, Tucker ES, Watson AT, Sertich JJW, Foster JR, Wiliams R, Garbe U, Bevitt JJ, Salvemini F. 2018. Neutron scanning reveals unexpected complexity in the enamel thickness of an herbivorous Jurassic reptile. J. R. Soc. Interface 15: 20180039. http://dx.doi.org/10.1098/rsif.2018.0039

Johnston PA. 1979. Growth rings in dinosaur teeth. Nature 278:635-636 doi 10.1038/278635a0.

Kear BP, Larsson D, Lindgren J, Kundrat M. 2017. Exceptionally prolonged tooth formation in elasmosaurid plesiosaurians. PLoS ONE 12(2): e0172759. Doi:10.1371/journal.pone.0172759

Khan B, Tansel B. 2000. Mercury Bioconcentration Factors in American Alligators (*Alligator mississippiensis*) in the Florida Everglades. Ecotoxicology and Environmental Safety 47: 54-58 doi:10.1006/eesa.2000.1923

Kieser JA, Klapsidis C, Law L, Marion M. 1993. Heterodonty and Patterns of Tooth Replacement in *Crocodylus niloticus*. Journal of Morphology 218: 195-201.

Klevezal GA. 1996. Recording structures of mammals. Determination of age and reconstruction of life history. CRC Press. Balkema, Rotterdam, Netherlands. [translation of 1988 book, cited version is the preprint]

Kosch JCD. 2014. Tooth replacement and dentition in *Giraffatitan brancai*. Unpublished Master Thesis. Pp 1-192

Lamm E.T. 2013, Preparation and Sectioning of Specimens. In: Padian K., Lamm E.T, editors. Bone Histology of Fossil Tetrapods. University of California Press; pp 55–160.

Lawson R, Wake DB, Beck NT. 1971. Tooth replacement in the red-backed salamander, *Plethodon cinereus*. Journal of Morhpology 134: 259-269

LeBlanc ARH, Reisz RR, Evans DC, Bailleul AM. 2016. Ontogeny reveals function and evolution of the hadrosaurid dinosaur dental battery. BMC evolutionary biology, 16, 152. doi:10.1186/s12862-016-0721-1

Neill WT. 1971. The Last of the Ruling ReptilesAlligators, Crocodiles and Their Kin, pp. 263-277. Columbia University Press, New York.

Osborn JW. 1970. New Approach to Zahnreihen. Nature 225: 343-346
Pike AVL, Maitland DP. 2004. Scaling of bird claws. Journal of Zoology 262: 73–81.

Osborn JW. 1975. Tooth replacement Efficiency, patterns and evolution. Evolution 29: 180-186.

Ricart RSD, Santucci RM, Andrade MB, Oliveira CEM, Nava WR, Degrazia GF. 2019. Dental histology of three notosuchians (Crocodylomorpha) from the Bauru Group, Upper Cretaceous, South-eastern Brazil, Historical Biology, DOI: 10.1080/08912963.2019.1675057

Richman JM, Whitlock JA, Abramyan J. 2013. Reptilian Tooth Regeneration. In Huang GT-J, Thesleff I. (Editors) Stem Cells in Craniofacial Development and Regeneration. Wiley-Blackwell, Hoboken, New Jersey, USA. Pp. 135-151.

Salakka S. 2014. Tooth Replacement of Euhelopus Zdanskyi [sic!] (Dinosauria: Sauropoda) and the Evolution of Titanosaurian Tooth Morphology. Uppsala universitet, Institutionen för geovetenskaper
Examensarbete E, Paleobiologi Examensarbete vid Institutionen för geovetenskaper ISSN 1650-6553 Nr 295. Masters Thesis at the Department of Earth Sciences Uppsala University
Published at Department of Earth Sciences, Geotryckeriet Uppsala University, Uppsala, 2014

Sattler F. 2014. Tooth replacement of the sauropod dinosaur *Tornieria africana* (Fraas) from Tendaguru (Late Jurassic, Tanzania). Unpublished Bachelor Thesis Pp 1-41

Schmiegelow AB, Sellers KC, Holliday CM. 2016. Ontogeny of Enamel Thickness in the Teeth of Alligator and its Significance for Crocodyliform Dental Evolution. The FASEB Journal 30(1) suppl
https://www.fasebj.org/doi/abs/10.1096/fasebj.30.1_supplement.779.8

Schwarz D, Kosch JCD, Fritsch G, Hildebrandt T. 2015. Dentition and tooth replacement of *Dicraeosaurus hansemanni* (Dinosauria, Sauropoda, Diplodocoidea) from the Tendaguru Formation of Tanzania. Journal of Vertebrate Paleontology 35(6): e1008134-2 Doi: 10.1080/02724634.2015.1008134

Sellers KC. Schmiegelow AB, Holliday CM. 2019. The significance of enamel thickness in the teeth of *Alligator mississippiensis* and its diversity among crocodyliforms. Journal of Zoology doi.org/10.1111/jzo.12707

Sereno PC, Wilson JA, Witmer LM, Whitlock JA, Maga A, Ide O, Rowe TA. 2007. Structural Extremes in a Cretaceous Dinosaur. PLoS ONE 2(11): e1230. Doi:10.1371/journal.pone.001230

Smith TM. 2004. Incremental Development of Primate Dental Enamel. Dissertation at Stony Brook University.

Westergaard B, and Ferguson MWJ. 1990. Development of the dentition in *Alligator mississippiensis*. upper jaw dental and craniofacial development in embryos, hatchlings, and young juveniles, with a comparison to lower jaw development. American Journal of Anatomy 187: 393- 421.

Whitlock JA, Richman JM. 2013. Biology of tooth replacement in amniotes. International Journal of Oral Science 5: 66-70

Wu XB, Xue H, Wu LS, Zhu JL, Wang RP. 2006. Regression analysis between body and head measurements of Chinese alligators (*Alligator sinensis*) in captive population. Animal Biodiversity and Conservation, 29.1: 65–71.

Wu Ping, Wu Xiaoshan, Jiang Ting-Xin, Elsey RM, Temple BL, Divers SJ, Glenn TC, Yuan Kuo, Chen Min-Huey, Widelitz RB, Chuong Cheng-Ming. 2013. Specialized stem cell niche enables repetitive renewal of alligator teeth. Proceedings of the National Academy of Sciences 110 (22): E2009-E2018; DOI: 10.1073/pnas.1213202110

Figures

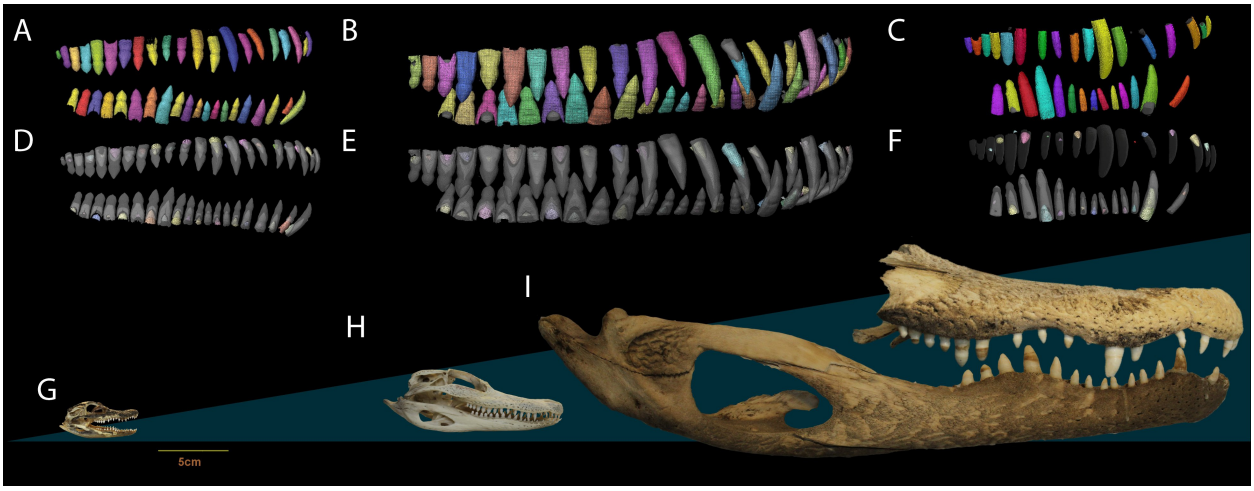

Figure 1. Dental anatomy of Alligator used in this study. (**A, D, G**) NCSM 100803; (**B, E, H**) NCSM 100804 and; (**C, F, I**) NCSM 100805. Segmented dentition showing (**A-C**) functional teeth in color and (**D-F**) replacement teeth in color. Replacement teeth and functional tooth of each position are presented in different shades of the same color, the coloration carries no additional meaning. Segmented dentition not to scale, skulls (**G-I**) to scale. Scale bar 5 cm.

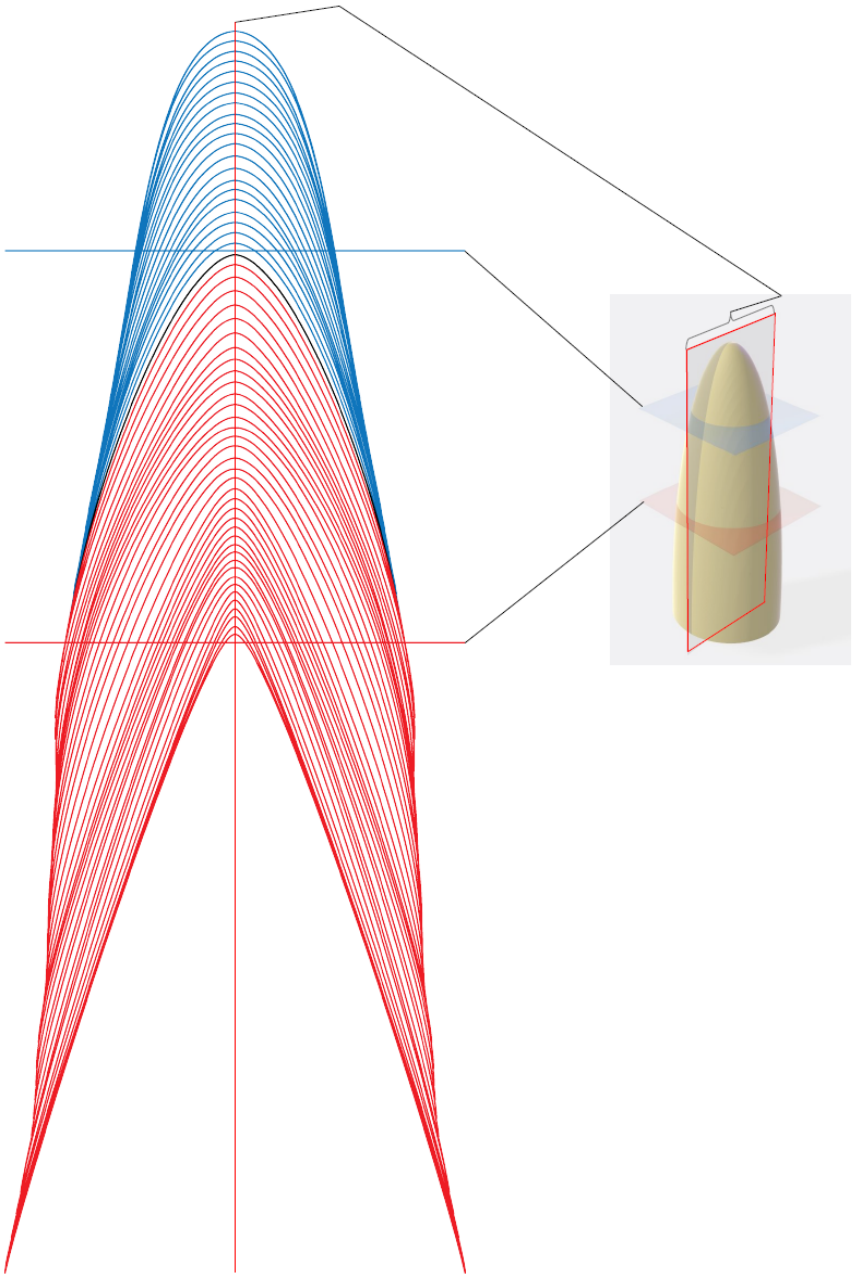

Figure 2. Schematic representation of section planes and transects. Schematic representation of different sectioning planes with examples of raw data for different transect locations. Blue VEL appear in transverse section taken in the blue plane. Red VEL appear in a transverse section in the red plane. A section in the plane of the CA (red with brackets) will cross all VELs.

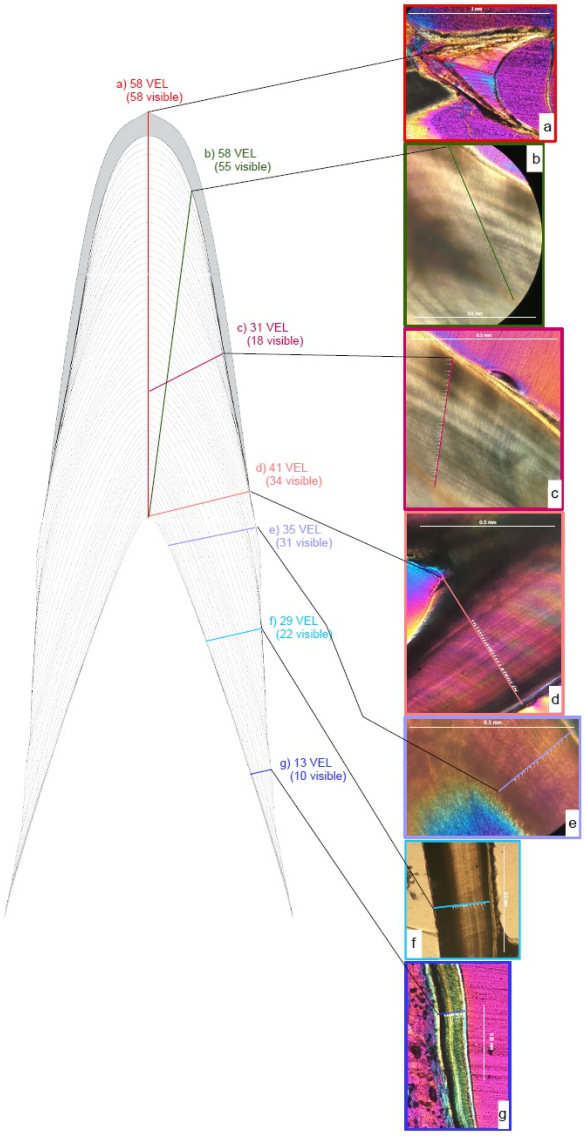

Figure 3. Schematic representation of transect orientations and examples. Schematic representation of different transect orientations. Transect orientations are represented by colored lines: a) base-apex transect along the CA from the tip of the pulp cavity to the crow apex representing CAH (red); b) near-crown-apex transect measured at the tooth apex, yet not along the CA (yellow-green); c) mid-crown transect measured in the central part of the crown (pink); d) crown base transect from the tip of the pulp cavity to enamel dentin junction (EDJ) almost perpendicular to the CA (salmon); e) root-base transect measured from the pulp cavity near the root base to the lateral dentin border (dark gray); f) mid-root transect measured from the pulp cavity at the mid root to the lateral dentin border (sky blue); g) root-apex transect measured from the pulp cavity near the root tip to the lateral dentin border (darker blue). Numbers next to the transects are the VEL crossed and the numbers visible under a hypothetical view through a microscope.

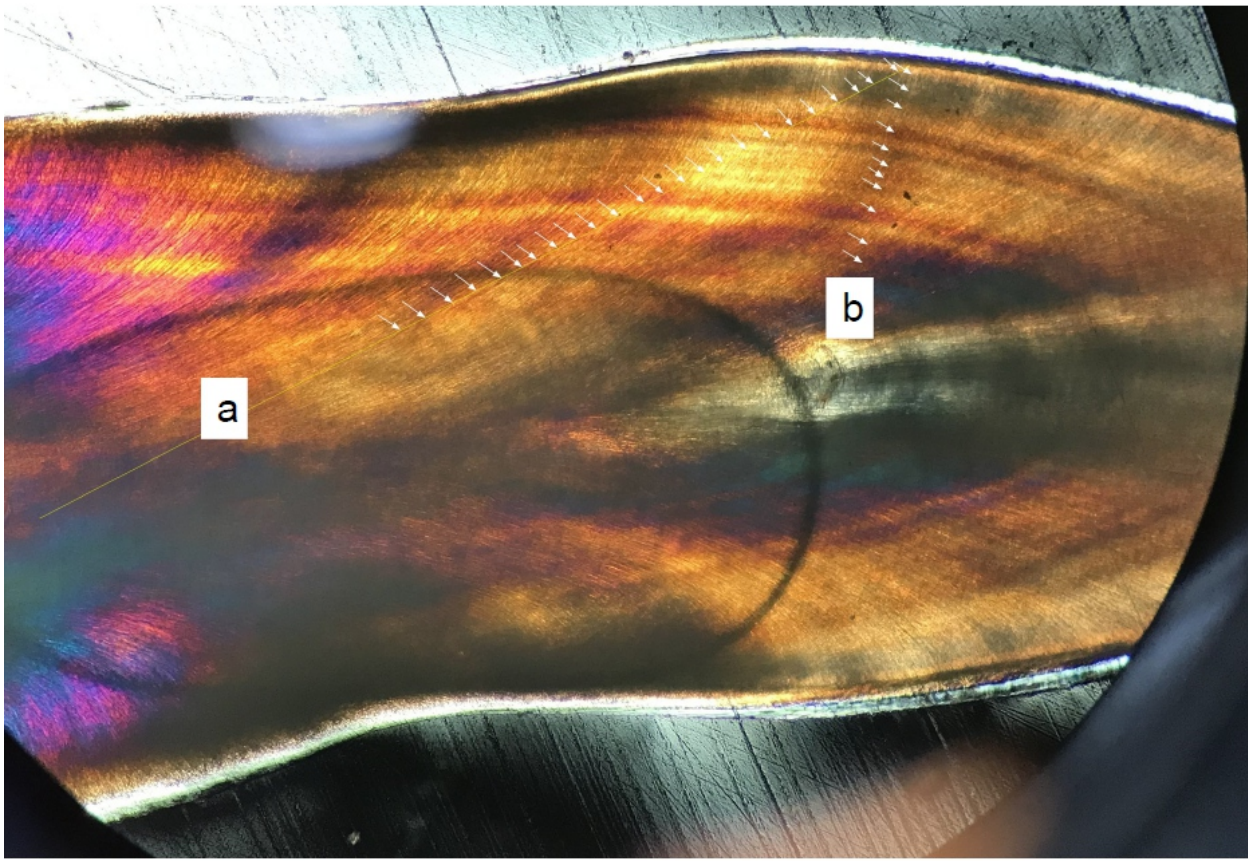

Figure 4. Oblique transect orientation. Yellow lines mark transects. Individual VEL are marked with arrows where they intersect with the transect: a) Transect strongly oblique to VEL, reaching from the crown base near the pulp cavity to the mid-crown (with no visible VEL in the medial position of the tooth); b) Transect perpendicular to VEL. Both transects derive from the first premaxillary alveolus of the medium sized alligator [NCSM 100804].

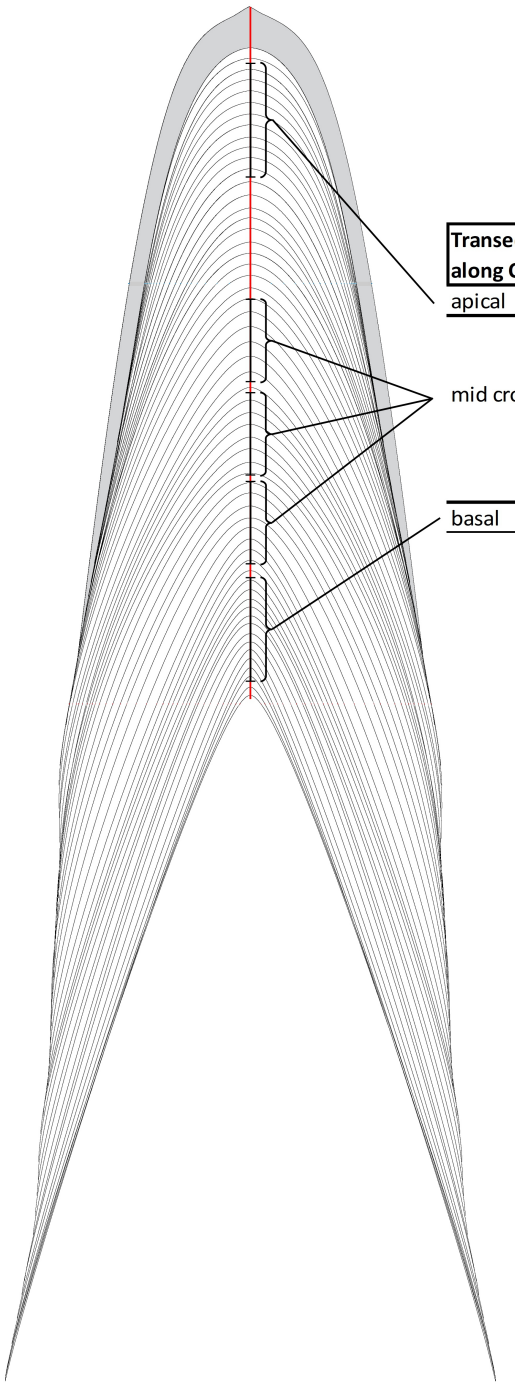

Transect position along CA of tooth	mean VEIW [µm]	SD	min	max	CH [mm]	TFT [days]
apical	16	4	10	30		314.1
	16	3	9	30		314.1
	17	3	10	24		295.6
mid crown	17	3	9	23	5.025	295.6
	18	4	11	30		279.2
	18	4	11	30		279.2
	17	4	7	29		295.6
basal	17	3	10	27		295.6

ANOVA: $F_{2, 473} = 7.52$ [$F_{crit} = 2.62$], $p < 0.05$ [0.0006]
Apical vs. mid: $q_{432} = 5.449$, $p < 0.05$ [0.000396]
Apical vs. basal: $q_{126} = 3.336$, $p < 0.05$ [0.04903]
Mid vs. basal: $q_{388} = 0.172$, $p > 0.05$ [0.992]
$q_{crit} = 3.325$

Figure 5. Examples of transects in different distances to pulp cavity. Schematic representation of transects in different distance to the pulp cavity. All transects are along the CA from the tip of the pulp cavity to the crown apex. All examples are from Dent 11 of the large specimen [NCSM 100805].

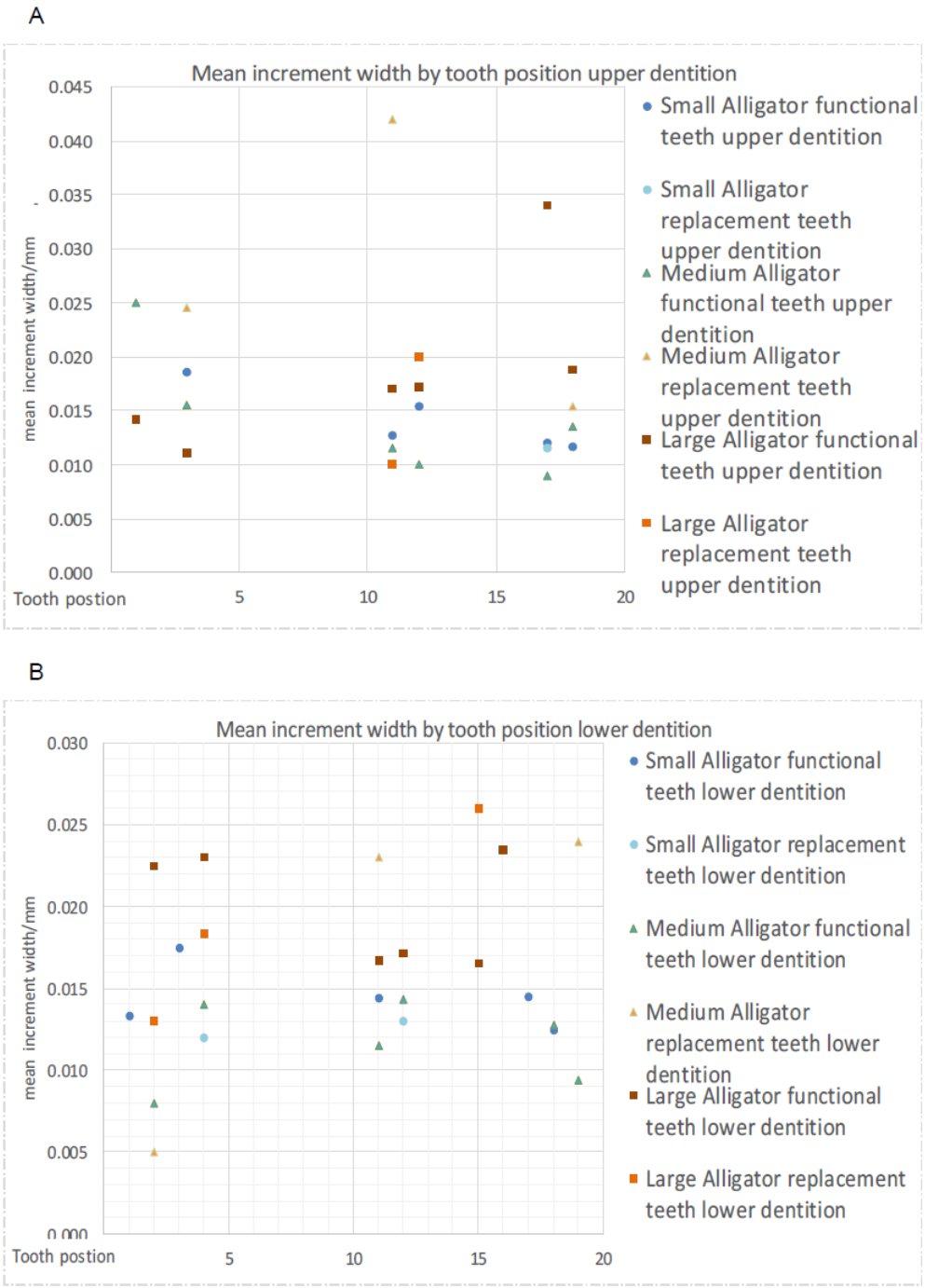

Figure 6. VEIW according to tooth position. Tooth position on the x axis, VEIW width in mm on the y axis. Each tooth position is depicted by its own point. A dentition of the upper jaw. B dentition of the lower jaw.

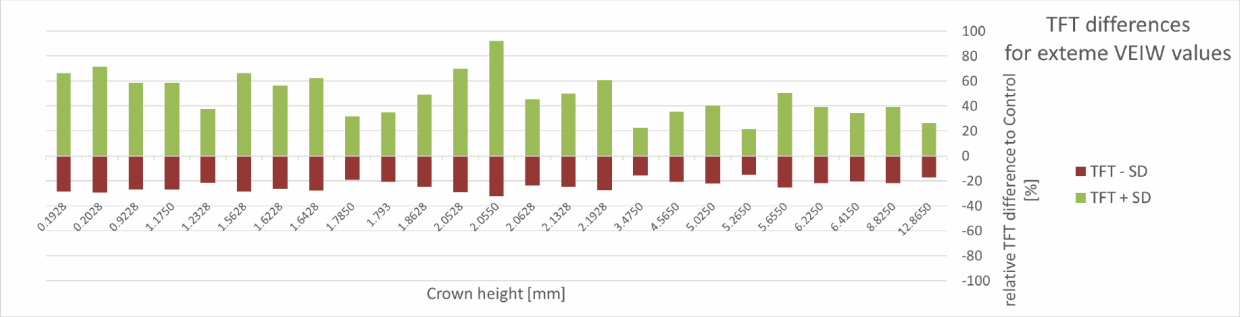

Figure 7. TFT differences for extreme VEIW values. For each tooth (on the x-axis with their crown height) the deviation of the upper and lower TFT estimate (upper estimate: based on mean VEIW [tooth] - 1 SD [grand mean]; lower estimate based on mean VEIW [tooth] + 1 SD [grand mean]) to the calculated TFTs [based on mean VEIW [tooth]) is shown in percent (see last two rows of table 4). Lower TFT estimates are in red-brown, upper TFT estimates in green.

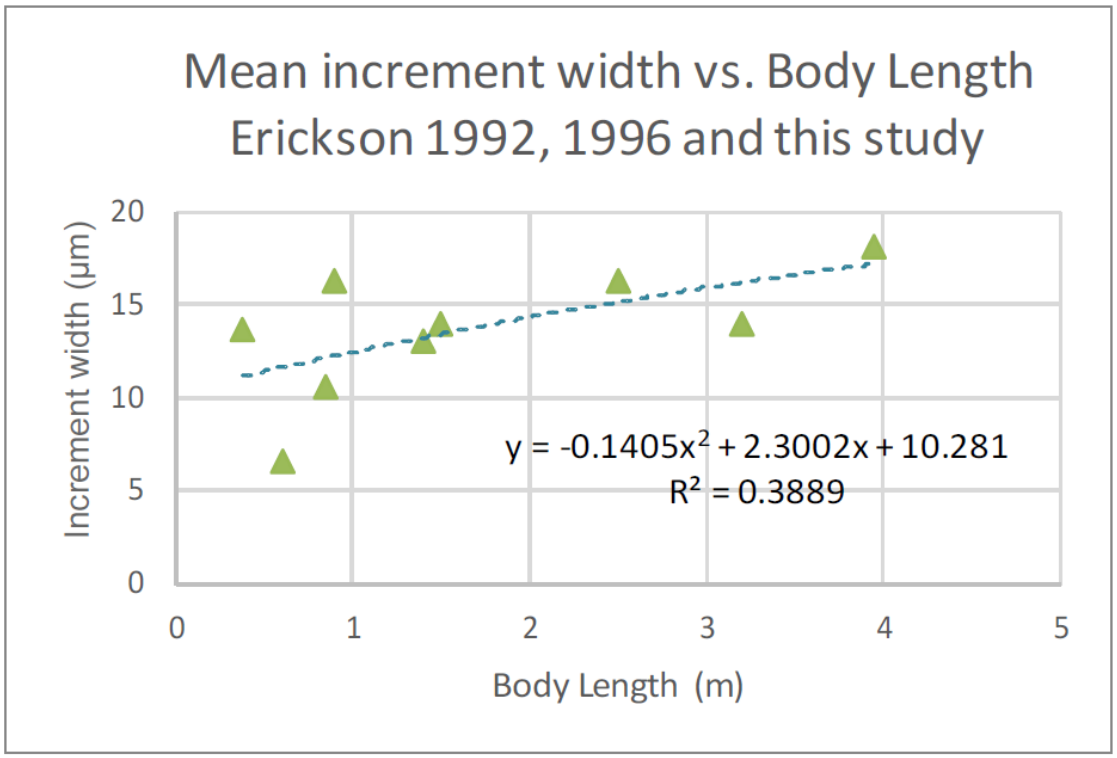

Figure 8. Mean specimen VEIW by body length. Mean VEIW vs. body length for *Alligator* specimens from this study and Erickson (1992, 1996a). The nearly linear shaped quadratic regression and the coefficient of determination are displayed.

Tables

Table 1. Transects oblique and perpendicular to VEL. Three pairs of measurements, each from the same tooth with one oblique and one perpendicular to the VELs and the resulting TFT for the tooth from applying them to CAH.

	oblique					perpendicular					
Tooth	**mean VEIW [µm]**	**SD**	**min**	**max**	**TFT [days]**	**mean VEIW [µm]**	**SD**	**min**	**max**	**TFT [days]**	**TFT difference**
Medium [NCSM 100804] Dent 18	21	5	12	34	118.45	14	4	8	21	177.68	59.22
Large [NCSM 100805] Dent 11	21	6	12	29	239.29	17.5	3	13	23.5	295.59	56.30
Large [NCSM 100805] Dent 11	22	6	12	36	228.41	16.5	3	12.5	21.5	304.55	76.14

Table 2. VEIW decrease in marginal VELs. Three examples of lateral transects other than the CA. Each has a subsample with a number of VELs close to the CA with their mean VEIW and a subsample of VEL furthest from the CA with their mean VEIW.

Tooth	**Transect**	**mean VEIW near CA [µm]**	**based on # VEL**	**TFT based on near CA VEIW**	**mean VEIW far CA [µm]**	**based on # VEL**	**TFT based on far CA VEIW**	**Difference in TFT estimates [%]**
Medium [NCSM 100804] Dent 18	mid crown	17.5	10	142.14	13.5	15	184.26	77.14
	mid crown	18.4	10	135.19	13.9	19	178.35	75.80
Large [NCSM 100805] Dent 4	root base	19.3	26	666.30	12.1	9	1062.25	62.73

Table 3. VEIW according to tooth position. Mean VEIW for the sampled tooth positions in mm. Only measurements with the same transect orientation were used (CA, excerpt for ' root base; * a combination of root base and crown base transects). Some tooth positions were sampled but had a different transect orientation from the other teeth and were excluded from table and analyses. Second generation replacement teeth (one in the dentition of the smallest specimen, four in the dentition of the medium sized specimen, three in the dentition of the largest specimen) are excluded. ANOVA result table for the three specimens. ANOVAs based on VEIWs of all sampled alveoli with a CA orientation and of just those alveoli with three or more CA samples below the table, using its values.

	Tooth position	1	2	3	4	11	12	15	16	17	18	19
Small Alligator NCSM 100803	functional teeth upper dentition			0.019		0.0127	0.0153			0.0120	0.0117	
	replacement teeth upper dentition									0.0115		
	functional teeth lower dentition		0.0133		0.0175		0.0144				0.0145	0.0125
	replacement teeth lower dentition				0.0120		0.0130					
Medium Alligator NCSM 100804	functional teeth upper dentition			0.0156*		0.0115*				0.009'	0.0135'	0.0094*
	replacement teeth upper dentition			0.0246		0.0370					0.0153	0.0240
	functional teeth lower dentition					0.0115*	0.0143*				0.0128*	
	replacement teeth lower dentition					0.0230						
Large Alligator NCSM 100805	functional teeth upper dentition	0.0143			0.0230	0.0170	0.0171				0.0188	
	replacement teeth upper dentition		0.0130		0.0183	0.0100	0.0200					
	functional teeth lower dentition					0.0167			0.0270			
	replacement teeth upper dentition							0.0260				

ANOVA for the three specimens						
	SS	df	MS	F	F crit	p
Between Groups	0.0001448	2	7.24235E-05	2.2953757	3.27	0.1156912
Within Groups	0.0011043	35	3.15519E-05		From F table for	
total	0.001249164	37			alpha = 0.05	
	overall	small	medium	large		
Mean	0.0163537	0.0137615	0.0170338	0.0184250		
SD	0.005810437	0.0022195	0.007989812	0.0050376		

ANOVA for all sampled alveoli in CA orientation						
	SS	*df*	*MS*	*F*	*F crit*	*p*
Between Groups	0.000367307	10	3.67307E-05	1.0416779	2.38	0.4481013
Within Groups	0.00066996	19	3.5261E-05		From F table for	
total	0.001037266				alpha = 0.05	

ANOVA for alveoli with 3 or more samples (4, 11, 12, 18)						
	SS	*df*	*MS*	*F*	*F crit*	*p*
Between Groups	5.67124E-05	3	1.89041E-05	0.4844291	3.29	0.6981058
Within Groups	0.000585353	15	3.90235E-05		From F table for	
total	0.000642065				alpha = 0.05	

Table 4. TFTs based on mean VEIW [tooth] ± 1 SD [grand mean]. TFTs based on mean VEIWs for the sampled tooth positions sorted by ascending CAH. Rows TFT ± SD show the TFT based on VEIW± SD [grand mean] derived for each tooth. TFT+ SD shows the mean VEIW [tooth] - 1 SD [grand mean] (TFT+ SD, as it produces bigger TFTs); TFT- SD shows VEIW [tooth] + 1 SD [grand mean] (TFT- SD as it produces smaller TFTs). SD ± [days] show the differences of TFT ± SD to the baseline TFT. Rows SD ± [%] are showing the same differences in percent (see also Fig 7). The last four columns show the mean TFT, the variance, t-test statistic and the p-value for a one sided two-sample t-test comparing TFT + SD and TFT - SD.

crown height [mm]	0.193	0.203	0.923	1.175	1.233	1.563	1.623	1.643	1.785	1.793	1.863	2.053	2.055	2.063	2.133	2.193	3.475	4.565	5.025	5.265	5.655	6.225	6.415	8.825	12.865	Mean	Variance	t-statistic	p-value
TFT by sampled CA sections [days]	16.067	17.635	70.985	90.385	70.446	130.233	121.710	131.424	89.250	96.908	128.469	175.954	205.500	134.530	148.111	173.116	133.654	249.000	301.500	195.000	396.842	364.035	342.133	519.118	559.348	194.454	20739.047		
VEIW of the tooth [mm]	0.012	0.012	0.013	0.013	0.018	0.012	0.013	0.013	0.020	0.019	0.015	0.012	0.010	0.015	0.014	0.013	0.026	0.018	0.017	0.027	0.014	0.017	0.019	0.017	0.023				
TFT + SD [days]	26.739	30.222	112.395	143.112	96.992	216.745	189.942	213.065	117.354	130.763	191.837	298.502	394.409	195.644	221.928	278.380	163.835	337.058	423.087	237.052	597.759	505.673	459.516	722.749	706.467	280.449	37706.375	1.7786	0.0411
TFT - SD [days]	11.483	12.450	51.873	66.050	55.308	93.081	89.544	95.016	72.006	76.978	96.570	124.742	138.948	102.510	111.143	125.616	112.863	197.423	234.197	165.620	297.012	284.381	272.519	405.009	462.942	150.211	13402.557	-1.1972	0.1187
SD + [days]	10.673	12.587	41.410	52.728	26.546	86.511	68.232	81.641	28.104	33.855	63.368	122.548	188.909	61.113	73.817	105.264	30.181	88.058	121.587	42.052	200.917	141.638	117.383	203.631	147.119				
SD - [days]	-4.583	-5.185	-19.112	-24.335	-15.138	-37.152	-32.166	-36.408	-17.244	-19.930	-31.899	-51.212	-66.552	-32.021	-36.968	-47.500	-20.791	-51.578	-67.303	-29.380	-99.831	-79.654	-69.615	0.000	-96.406				
SD + [%]	66.428	71.378	58.337	58.337	37.683	66.428	56.061	62.120	31.490	34.935	49.326	69.648	91.926	45.427	49.839	60.806	22.582	35.365	40.327	21.565	50.629	38.908	34.309	39.226	26.302				
SD - [%]	-28.528	-29.403	-26.924	-26.924	-21.488	-28.528	-26.429	-27.703	-19.321	-20.566	-24.830	-29.105	-32.385	-23.802	-24.960	-27.438	-15.556	-20.714	-22.323	-15.067	-25.156	-21.881	-20.347	-21.981	-17.235				

Table 5. Error margins for published TFTs . Published TFTs from Erickson (1996b), Graica and Zurriaguz (2016), and D'Emic et al. (2019b) ± one standard deviation (SD) based on relative SD. Central axis height was not included in the original publications and was back calculated based on mean VEIWs given in the publications. The last two columns are showing just the differences of TFT from VEIW±SD to mean TFT.

Taxon	Mean increment width, µm	Central axis height (from mean VEIW and TFT), mm	Mean tooth formation time, days	VEIW SD based on Alligator, µm	TFT + SD	TFT - SD	SD +	SD -	Source
Crocodilian	13	3.198	246	3.8916	351.1046	189.3248	105.1046	-56.6752	Erickson 1996b
Leidyosuchus	19	5.377	283	5.6877	403.9131	217.8005	120.9131	-65.1995	
Adult *Edmontonia*	13.5	3.7665	279	4.0413	398.2040	214.7221	119.2040	-64.2779	
Adult *Triceratops*	15.8	6.0198	381	4.7298	543.7840	293.2226	162.7840	-87.7774	
Infant Lambeosaurinae	11	1.617	147	3.2929	209.8064	113.1331	62.8064	-33.8669	
Adult *Prosaurolophus*	16	5.168	323	4.7897	461.0032	248.5850	138.0032	-74.4150	
Infant *Maiasaura*	12	1.584	132	3.5923	188.3976	101.5889	56.3976	-30.4111	
Adult *Maiasaura*	13	3.653	281	3.8916	401.0585	216.2613	120.0585	-64.7387	
Juvenile *Edmontosaurus*	14	3.15	225	4.1910	321.1323	173.1629	96.1323	-51.8371	
Adult *Edmontosaurus*	19.8	6.7122	339	5.9272	483.8393	260.8988	144.8393	-78.1012	
Adult *Deinonychus*	10.1	4.1713	413	3.0235	589.4562	317.8502	176.4562	-95.1498	
Adult *Troodon*	11	3.993	363	3.2929	518.0934	279.3696	155.0934	-83.6304	
Juvenile Albertosaur	14.5	4.9155	339	4.3406	483.8393	260.8988	144.8393	-78.1012	
Adult Albertosaur	14	7.266	519	4.1910	740.7451	399.4292	221.7451	-119.5708	
Juvenile *Tyrannosaurus*	14	3.696	264	4.1910	376.7952	203.1779	112.7952	-60.8221	
Sub. Ad. *Tyrannosaurus*	14	4.396	314	4.1910	448.1579	241.6585	134.1579	-72.3415	
Adult *Tyrannosaurus*	17	15.861	933	5.0890	1331.6286	718.0490	398.6286	-214.9510	
Titaosauria indet.	18.2	1.1648	64	5.4482	91.3443	49.2552	27.3443	-14.7448	Garcia
MPCA-Ph 4, 5, 9, 13, 19	20.8	1.1232	54	6.2266	77.0717	41.5591	23.0717	-12.4409	& Zurriaguz 2016
Majungasaurus									D'Emic et al.
FMNH PR 2100 Pmx dext 3	17.5510	5.12489	292	5.2540	416.7583	224.7270	124.7583	-67.2730	2019b
UA 9944 Mx sin 1	17.5510	4.63346	264	5.2540	376.7952	203.1779	112.7952	-60.8221	
FMNH PR 2100 Dent dext 2	17.5510	4.38775	250	5.2540	356.8137	192.4033	106.8137	-57.5967	
Ceratosaurus									
BYU 12893 Mx dext 6	14.4645	4.83115	334	4.3300	476.7030	257.0508	142.7030	-76.9492	
Allosaurus									
BYU 8901 Pmx dext 2	23	8.05	350	6.8851	499.5391	269.3646	149.5391	-80.6354	
BYU 8901 Mx dext 6	23	7.36	320	6.8851	456.7215	246.2762	136.7215	-73.7238	
BYU 2028 Dent sin 5	23	8.165	355	6.8851	506.6754	273.2127	151.6754	-81.7873	

Table 6. Impact of VEIW±1SD on TFT and TRR of sauropods. Ranges of mean tooth formation times (TFTs) for tooth positions of the sauropods *Diplodocus* sp., *Camarasaurus* sp., *Torneria africana*, *Giraffatitan brancai*, *Brachiosaurus* sp., and *Dicraeosaurus hansemanni* and resultant tooth replacement rates (TRR) based on TFT from VEIW±1SD. D'Emic et al. (2013, 2019a) only give TFT for some teeth, so the full range of TFTs found in the position is displayed, for other tooth positions the mean TFT found in this position in the jaw element is displayed. For explanation of TRR, TRR max-max, TRR min-min, TRR min-max, TRR max-min see methods.

Taxon	tooth position	Mean tooth formation time, days	TFT + SD	TFT - SD	TRR (count)	TRR max-max	TRR min-min	TRR min-max	TRR max-min	Source
Diplodocus YPM 4677	I	187 - 183	264.0421	142.37843						D'Emic et al. 2013
pmx	II	178 - 145	230.50162	124.29252	36	51.3811662	27.7060719	-67.323126	146.410364	
Average for tooth postion	III	144 - 113	189.34911	102.10201	33	47.0994023	25.3972326	-47.929795	120.42643	
	IV	110	156.99801	84.657442						
Camarasaurus UMNH 5527	I	130 - 113	173.41144	93.507993						
pmx	II	315 - 208	373.22708	201.25383	62	88.4897862	47.7160128	-118.66729	254.873088	
Average for tooth postion	III	253	361.09542	194.71212	63	89.9170408	48.4856259	-76.46626	214.868927	
	IV	190	271.17838	146.22649	60	85.635277	46.1767865	-39.316609	171.128673	
Tornieria aficana MB.R.2345	I									Sattler 2014
mx sin	II	135.23333	193.0124	104.07735						
Average for tooth postion	III	148.925	212.55389	114.61463						
MB.R.2346	I	156.325	223.11558	120.30977						
pmx sin	II	118.6	169.2724	91.276115	37.725	53.8431804	29.0336545	-48.962628	131.839463	
	III	102.66667	146.53147	79.013613	17.95	25.6192204	13.8145553	-56.585968	96.0197437	
MB.R.2343	II	125.775	179.51295	96.798089	36.875	52.630014	28.3794834	-54.335377	135.344875	
pmx dext	III	96.4	137.58735	74.190704						
Giraffatitan brancai	I	216.34185	308.7749	166.49952						Kosch 2014
MB.R.2180.1	II	229.58588	327.6775	176.6923	73.45515	104.839202	56.5320464	-47.640045	209.011294	
pmx sin	III	158.40255	226.08077	121.90868						
MB.R.2181.1	I	286.51966	408.9365	220.50928	91.429944	130.493809	70.3656834	-57.93341	258.792903	
pmx sin	II	202.47359	288.98137	155.82633	64.141313	91.5459848	49.3639952	-41.609053	182.519033	
	III	138.33228	197.43538	106.46234						
MB.R.2181.2	I	279.67743	399.17091	215.24342	58.546766	83.5611426	45.0583589	-100.36635	228.985847	
pmx dext	II	221.13067	315.60976	170.18506	89.172642	127.272065	68.6284342	-27.342551	223.24305	
	III	145.93207	208.28222	112.31123						
MB.R.2180.2	I									
mx sin	II	205.04286	292.64837	157.80367	92.5302	132.064155	71.2124549	-16.15397	219.43058	
first 5 alveoli	III	132.8481	189.60806	102.24164						
MB.R.2180.3	I	132.8481	189.60806	102.24164						
mx dext	II	178.00815	254.06295	136.99741	80.6809	115.152187	62.0930783	-20.213781	197.459047	
first 5 alveoli	III	139.7876	199.5125	107.58237						
MB.R.2181.4	I	132.8481	189.60806	102.24164						
mx sin	II	178.00815	254.06295	136.99741	80.6809	115.152187	62.0930783	-20.213781	197.459047	
first 5 alveoli	III	139.7876	199.5125	107.58237						
MB.R.2181.3	I	211.37094								
mx dext	II	224.10303	319.85209	172.47263	74.067571	105.713282	57.0033733	-40.618237	203.334892	
first 5 alveoli	III	146.13906	208.57765	112.47054						
MB.R.2180.14	I									
dent sin	II	227.88582	325.25109	175.38391	114.2043	162.998614	87.8931264	-6.7548695	257.64661	
first 5 alveoli	III	143.92035	205.41098	110.76299						
MB.R.2180.13	I									
dent dext	II	236.83206	338.01965	182.26906	104.13811	148.631604	80.1460577	-19.387186	248.164848	
first 5 alveoli	III	154.93029	221.12497	119.23638						
***Brachiosaurus* sp.** USNM 5730	I	280	399.81469	215.59057	52.8825	75.4767922	40.6990652	-108.74734	224.923194	D'Emic et al. 2019a
mx	II	260-227	350.68635	189.09928	97.5935	139.290773	75.109237	-28.366643	242.766653	
Average for tooth postion	III	162-153	224.56981	121.09393						
dent	I	258-242	358.57528	193.35319	83.715125	119.482799	64.4282576	-45.739289	229.650345	
Average for tooth postion	II	185-150	239.09248	128.92493						
Dicraeosaurus hansemanni	I									Kosch 2010,
MB.R.2337	II	188.5	269.0375	145.07207	20.333333	29.0208439	15.6487999	-95.931043	140.600686	Schwarz et al. 2015
pmx dext	III	174	248.3423	133.91268	34.666667	49.47816	26.6799211	-62.101682	138.259764	
	IV	141	201.2429	108.51545	60.333333	86.1110285	46.4333242	-2.670575	135.214928	
	V	74.75	106.68728	57.52858	76	108.471351	58.4905963	39.4189926	127.542955	
	VI	28.5	40.676757	21.933974						

Table 6. (continued)

MB.R.2338	I									
pmx sin	II	185.25	264.39892	142.57083	19	27.1178377	14.6226491	-96.847586	138.588073	
	III	175.25	250.12637	134.8747	54	77.0717493	41.5591079	-38.234728	156.865585	
	IV	123.25	175.90913	94.854816	50.666667	72.3142339	38.9937309	-7.4796023	118.787567	
	V	65.25	93.128364	50.217255	77	109.898605	59.2602094	38.2156812	130.943134	
	VI	32	45.672148	24.627619						
MB.R.2339	I									
pmx sin	II	189	269.75112	145.45688	10	12.8452915	6.92651798	-111.77777	131.549584	
	III	181.75	259.40353	139.87718	43.25	61.7287622	33.285767	-57.797582	152.812111	
	IV	138.5	197.67476	106.59142	58.25	83.1375814	44.8299636	-7.9457673	135.913312	
	V	80.25	114.53718	61.761452	56.5	80.6398858	43.4831407	28.357386	95.7656405	
	VI	23	32.826856	17.701102						
MB.R.2336	I									
max dext	II	176	251.19681	135.45191	35.25	50.3107252	27.1288621	-65.43418	142.873767	
first 5 alveoli	III	149	212.66094	114.67235	62.75	89.5602272	48.2932226	-14.182721	152.03617	
	IV	95	135.58919	73.113245	55.25	78.8558175	42.5211243	16.3798744	104.997067	
	V	38.6	55.092028	29.707066						
MB.R.2371	I									
dent sin	II	153.4	218.94086	118.05865	49.6	70.791829	38.1728102	-30.090378	139.055017	
first 5 alveoli	III	103.8	148.14903	79.885841	61.6	87.9188844	47.4081675	19.6556959	115.671356	
	IV	42.2	60.230145	32.477673						

APPENDICES

Appendix A

Sampling impact assessments of Tooth Growth and Replacement Rates in Archosaurs: implications for Paleontological Studies, Supplemental 1

Kosch, Jens[1,2]
Zanno, Lindsay[1,2]

1. Department of Biological Sciences, North Carolina State University, Raleigh, NC, USA
2. Paleontology, North Carolina Museum of Natural Sciences, Raleigh, NC, USA

Transect orientation and the effects of sampling location for on VEIW measured in a tooth

We refute the assumption that mean von Ebner increment width (**VEIW**) is consistent regardless of the transect position used for sampling. There are two aspects to the effect of transect orientation: 1) transects oriented perpendicular to von Ebner lines (**VELs**) but variable in tooth location (with regard to the tooth from root to apex), and 2) transect orientation relative to VEL trendlines (perpendicular or obliquely oriented).

With regard to location on the tooth, sections that do not precisely section the central axis (**CA**) do not preserve all VELs. Figure 1 of Erickson (1992) (redrawn in Fig. 1b) and Figure 2 of the main text illustrate sections through the CA. Transverse sections omit VELs, particularly those of the crown apex (Fig. 1a). VEL counts along mesiodistal or labiolingual transects (lateral to the pulp cavity) are consistently fewer than those derived from a CA transect (upwards of 40%). Erickson (1992) outlines a method to avoid missing those lines in pure line counts, by tracing the last clearly visible VEL further to the crown apex and starting a new transect from that VEL (which can be repeated as many times as necessary to record all VEL of the tooth). The zig-zag pattern following the last visible VEL to a further apical position allows to count all VEL in the tooth (Fig. 1b)

However, this method does not consistently record VEIWs of the same relative position, so mean VEIW obtained from these counts (as done by Erickson [1992]) will be diminishing the further laterally from the CA the VEL are positioned (see the distance between duplicated VEL crossed in the basal and apical transect in Fig. 1). We find that mean VEIW in a tooth decreases laterally (Fig. 1, Fig. 2) even when sampled perpendicular to VEL trendlines; VEIWs are thickest along the CA from above the pulp cavity to the crown apex and thinnest when taken as true transverse planes near the enamel dentin junction (**EDJ**). Transects along the CA yield a more constant VEIW due to not measuring the laterally decreasing width of VEIW while also keeping the transect perpendicular to the VEL (Fig. 1a).

However, variation in VEIW is less affected by transect location as it is by transect orientation relative to VEL trendlines. Transects that cross VELs obliquely (Fig. 3) (e.g., top of the pulp cavity to the EDJ, in areas adjacent to the apex (Fig. 3b in the main text) yield VEIWs up to nearly twice the width than those made perpendicular to VEL trendlines (this is average from some test measurements [Fig. 4], the exact value depends on the orientation [angle] of the trendline to the VELs; see also table 2

in the main text). This variation results in differential calculations of TFT depending on transect orientation.

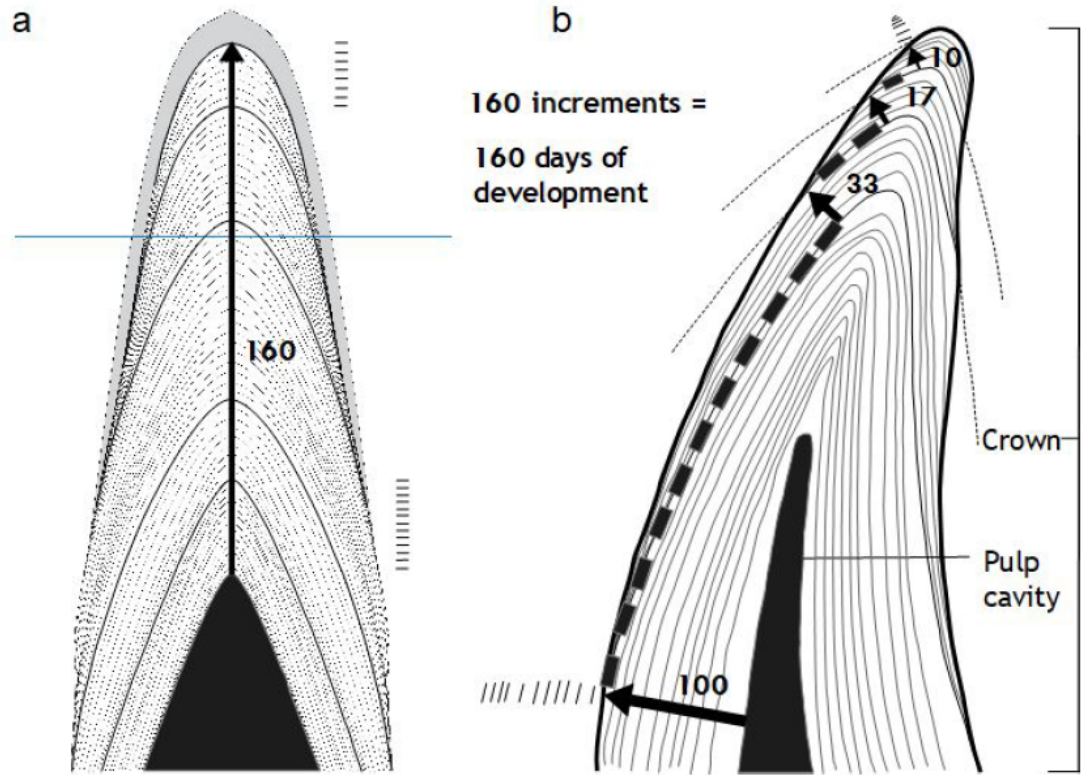

Fig. 1 Different schemes for transects to count VELs and influence on VEIW
Areas with arrows are the transects. VEL of the lowest and the topmost sections are duplicated outside thee tooth. **a** Transect through CA, counting all VEL in one transect (arbitrary set to 160, as in Erickson [1992] Fig. 1) with a more constant VEIW due to not measuring the laterally decreasing width of VEIW while also keeping the transect perpendicular to the VEL. **b** Figure 1 from Erickson (1992) redrawn with minor changes in VEL depiction.

Ontogenetic scaling of VEIW

When we derive mean VEIW across the whole dentition of our sampled individuals (from smallest to largest: NCSM 100803, NCSM 100804, and NCSM 100805), we find a slight increase during ontogeny (Fig.5a); however, three individuals are not enough for a meaningful statistic comparison. To our data, we added the mean VEIW of differently sized *Alligator* specimens ranging in body length from 0.60 m to 3.20 m from Erickson (1992 and 1996a) (Fig. 5b). We find the relationship between VEIW and body length does not reach 95% significance ($p = 0.0738$) but find an ontogentic signal ($R^2 = 0.3889$). Thus, it seems likely that there is no reliable trend of increasing VEIW during ontogeny, that needs to be taken into account when applying mean VEIW across growth series to derive TFT. Erickson 1996a adds data points for TRR of hatchling *Alligator* to his Fig. 3 and Erickson

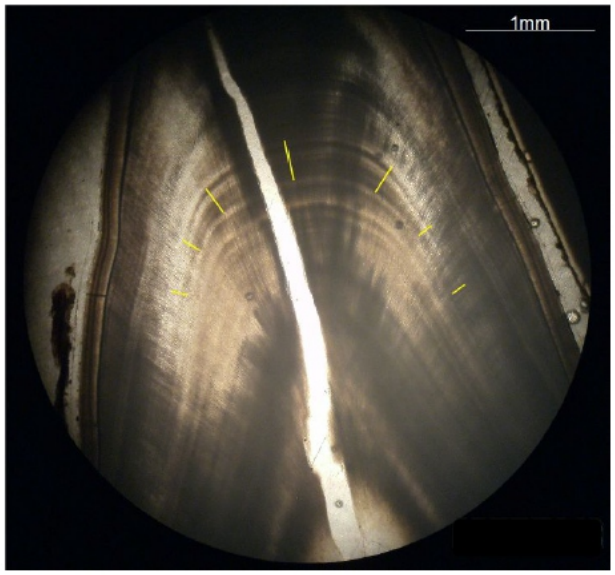

Fig. 2 Variation of Increment Line Thickness within a Tooth
Yellow lines mark the same group of incremental growth lines. The height of these lines is decreasing lateral to the CA.

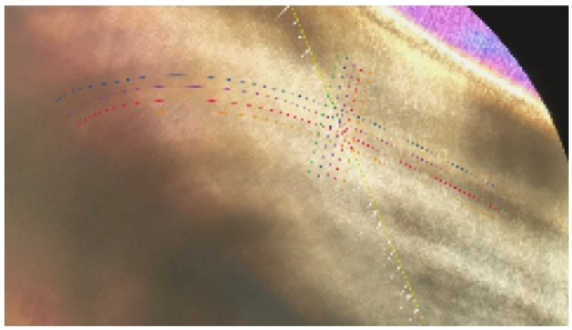

Fig. 3 VEIW in oblique transects
The straight Yellow line is the transect. The individual VEL are marked with arrows where they intersect with the transect. Select neighboring VEL are accentuated by blue, purple, red, and organge lines. Lines in the same colors and green are showing an orientation perpendicular to the VEL. Sections of the transect line crossing between the accentuated VELs are marked by the corresponding colors.

However, as outlined in the previous section, Erickson (1992, 1996a) used a zig-zag method when counting VEIW, which leads to a systematic underestimation of mean VEIWs by conflating lateral VEIWs measured far from the CA with wider VEIWs measured closer to the CA.
We performed a preliminary correction for reported VEIWs of Erickson (1992, 1996a) by adding 26.667% to the reported width (following the assumption that 1/5 of the transects used by Erickson are using VEIWs that are 33% too short). This does increase the correlation of body length to specimen mean VEIW to a more significant value (OLS regression $p < 0.05$ [$p = 0.0455$], $R^2 = 0.457$; $R^2 = 0.680$ for a quadratic regression) (Fig. 6, table 1). However, we do not deem this ad hoc correction of Erickson's (1992, 1996a) mean VEIWs precise enough to confidently apply it to all of his measurements obtained from Erickson's zig-zag counting and measuring method (e.g. in table 5 of the main text).
Our preliminary assessment is that VEIW does not change systematically during ontogeny, making it possible to apply mean VEIWs obtained to various ontogenetic stages of a species without introducing an ontogenetic scaling factor.

Tooth age by tooth and crown height
If all three individuals of different ontogenetic status are treated as a single sample there is a significant correlation between TFT calculated from VEIWs and central axis height (**CAH**) and tooth height (**TH**) [$p = 5.56291E-19$ and $p = 7.66367E-12$ respectively], but the coefficient of determination R^2 of the corresponding linear regressions is low for the relationship with TH (0.6345 and 0.8175 respectively, see Fig. 7). If other types of function are used for TH even the best result (a function of the type $y = k\ x^a$) only explains 80.46% of the spread of the data (Fig. 8a). If the three individuals are treated separately

(Fig. 8b), the small alligator's tooth age can be sufficiently described by various transfer functions (those with the highest coefficient of determination are displayed in Fig. 8b), but in the medium sized alligator only CAH shows a significant correlation to TFT (which is in part circular reasoning, as TFTs based on the crown height and tooth specific VEIWs) and the fit to the data spread is not very good ($R^2 = 0.49$ for a function of the type $y = k\ x^a$) and the large alligator has a significant relationship between tooth age and either tooth height ($R^2 = 0.73$, for an exponential function as an approximation) or crown height ($R^2 = 0.82$, for a quadratic function).
This lack of a fitting transfer function for the medium sized individual should serve as a caveat for constructing tooth-height-tooth-age relationships sensu D'Emic et al. (2013), based on lower quality VEIW measurements with few measured VEL and multiple different orientations of the transect axis.

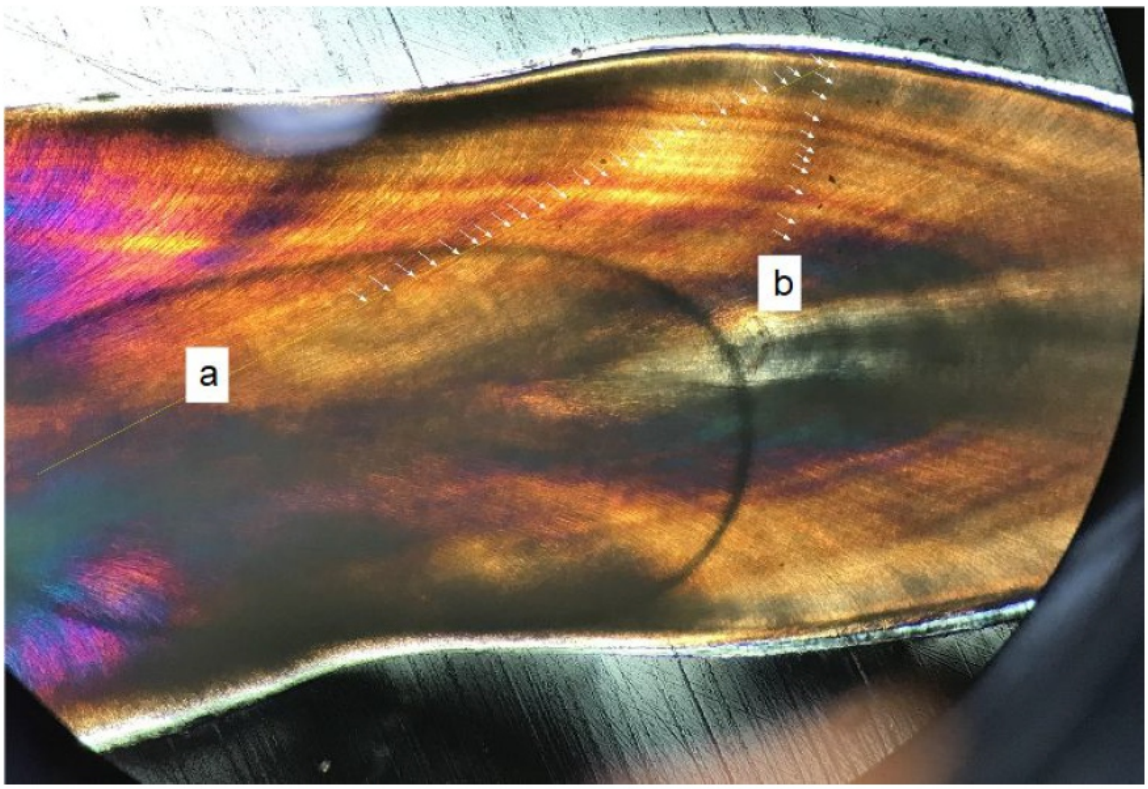

Fig. 4 Oblique transect orientation
The straight yellow line is the transect. Arrows denote the intersection of the VELs with the transect. Transect a is strongly oblique to the VEL and reaches from the crown base near the pulp cavity to the mid-crown. Transect b meets the VEL in perpendicular fashion, but includes only the VEL a transverse section would have. From the first premaxillary alveolus of the medium sized alligator [NCSM 100804].

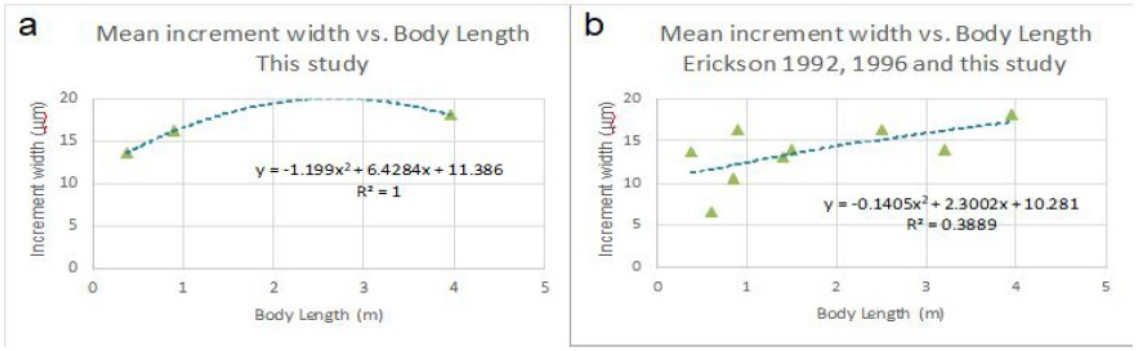

Fig. 5 Mean VEIW of individuals during ontogeny of *Alligator*
a Mean VEIW vs. body length for specimens in this study. **b** Mean VEIW vs. body length for this study and Erickson (1992, 1996). Both of the plots seem to suggest a slight increase of VEIW in ontogeny, but the plot with nine specimens establishes that the fit of the trend is not good ($R^2 = 0.39$) and the correlation for an OLS regression is not significant ($p = 0.0738$)

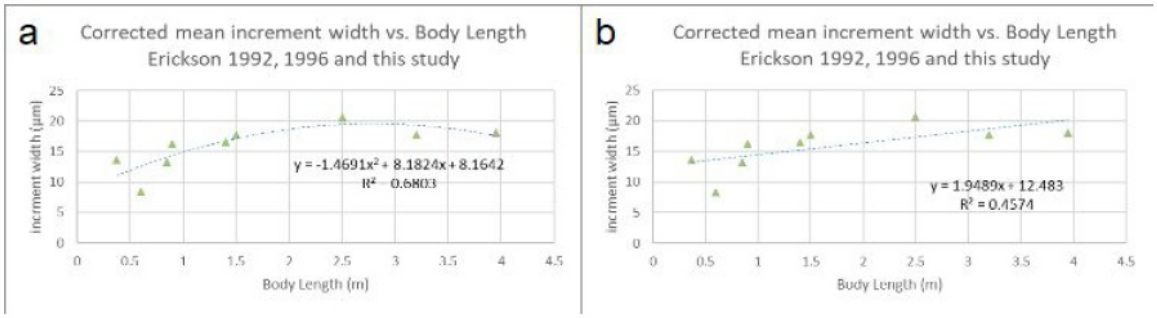

Fig. 6 Corrected mean VEIW of individuals during ontogeny of *Alligator*
a Corrected mean VEIW vs. body length for specimens in this study and Erickson (1992, 1996a with quadratic regression. **b** Corrected mean VEIW vs. body length for this study and Erickson (1992, 1996a) with a OLS regression. Both of the plots seem to suggest a slight increase of VEIW in ontogeny, but the coefficient of determination better fits a quadratic regression ($R^2 = 0.68$) than for the linear regression ($R^2 = 0.46$) and the correlation for an OLS regression is significant ($p = 0.0455$).

Table 1 VEIW and TRR in relationship to body size

Mean VEIW as reported by Erickson (1992, 1996b) or obtained from our study. Mod. VEIW is reported VEIW multiplied by 1.2667 (see text for explanation). P values are from an OLS regression.

	Body length (m)	Sample size	Mean tooth replacement rate (days)	mean VEIW (µm)	mod. mean VEIW
This study	0.37	1	87.0467	13.6	13.6
Erickson 1996	0.6	2	83	6.6	8.36
Erickson 1996	0.85	2	109	10.5	13.3
This study	0.9	1	133.6184	16.2	16.2
Erickson 1996	1.4	2	122	13	16.467
Erickson 1992	1.5	?	115	14	17.733
Erickson 1992	2.5	?	154	16.3	20.647
Erickson 1992	3.2	?	260	14	17.733
This study	3.95	1	278.9975	18.07	18.07

	R^2	p value	mod. R^2	mod. p value
VEIW All data	0.387	0.0738	0.457	0.0455
VEIW Erickson 1996 & this study	0.057	0.698	0.36	0.2852
VEIW Erickson 1996	0.89	0.2157	0.89	0.2157
VEIW This study	0.787	0.3056	0.787	0.3056
replacement rate all alligators	0.902	9E-05	0.902	9E-05
replacement rate this study	0.991	0.0618	0.991	0.0618
replacement rate all + Erickson 1992	0.886	2E-05	0.886	2E-05
replacement rate all + Erickson 1996	0.896	1E-05	0.896	1E-05

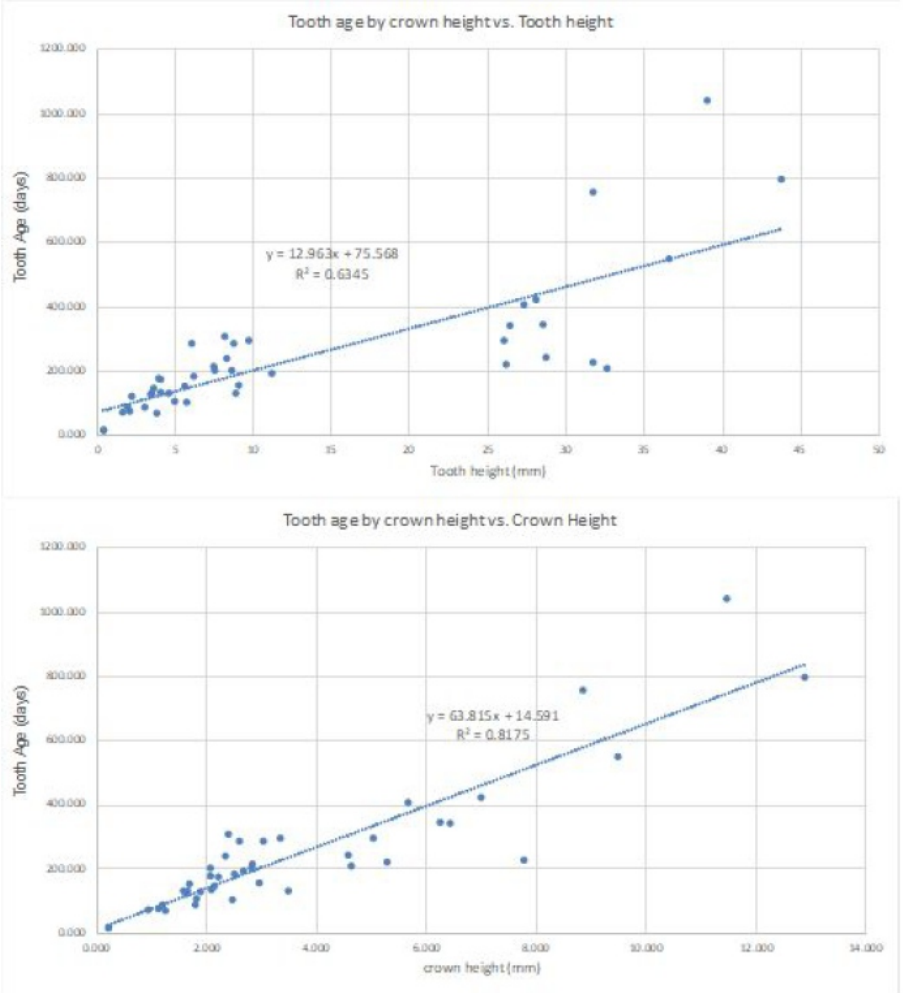

Fig. 7 Tooth age of *Alligator* to TH and CAH with linear trendlines

Tooth age derived from mean VEIW (=TFT) of individual teeth and CH plotted against TH and CAH with linear trendlines. All three *Alligator* specimens in the study are treated as one dataset for these.

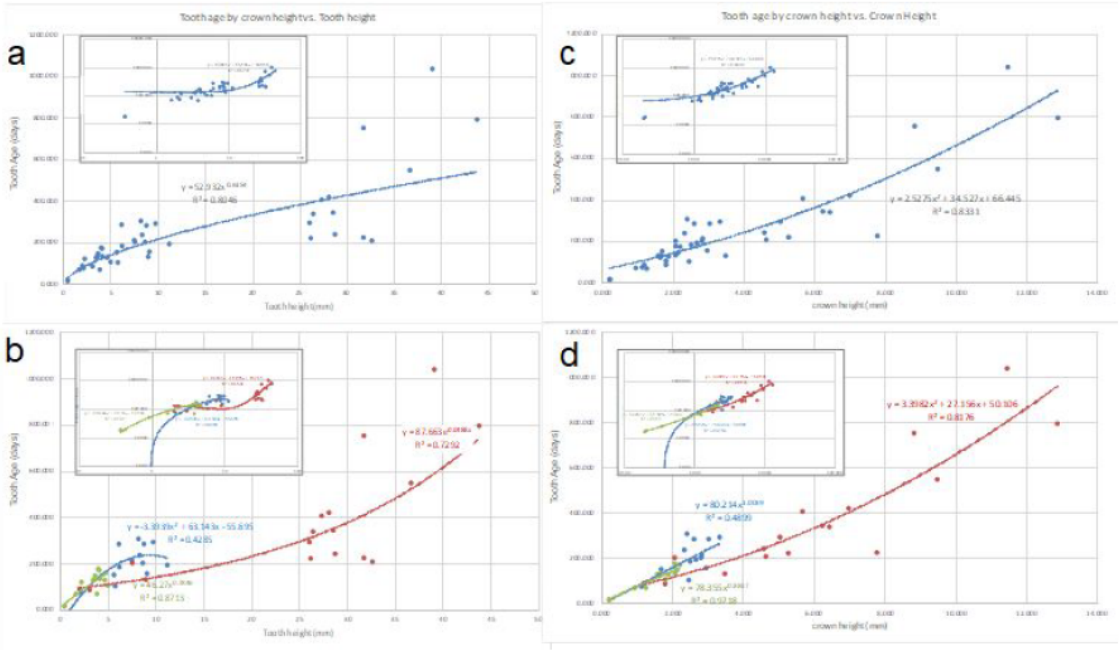

Fig. 8 TFT of *Alligator* to TH and CH with the best supported trends
a & **b** TH to TFT; **c** & **d** CAH to TFT. **b** & **c** show a treatment of the three specimens as three different datasets, **a** & **c** a treatment that treats all teeth as the same dataset. Small insets show the respective plots in a logarithmic scale and consistently use polynomes of the second order for the trendlines. **a** uses a function of the type $y = k\ x^a$. In **b** the small *Alligator* (NCSM 100803) uses a function of the type $y = k\ x^a$. The medium sized specimen (NCSM 100804) uses a polynome of the second order for the trendline. The large sized specimen (NCSM 100805) uses an exponential function for the trendline. **c** uses a polynome of the second order for the trendline. In **d** the small (NCSM 100803) and the medium sized specimen (NCSM 100804) use functions of the type $y = k\ x^a$. The large sized specimen (NCSM 100805) uses a polynome of the second order (= quadratic function) for the trendline.

Scaling of tooth replacement rate
Tooth replacement rate was derived from mean VEIW of the teeth and CAH, so it combines those observations, and when viewed in an ontogenetic context shows mainly the impact of tooth size (and thus CAH) increase.
When mean replacement rates for upper and lower dentition are observed it appears that mean central axis height (CAH) of the upper dentition is greater and replacement rate is slower in the medium (NCSM 100804) and large (NCSM 100805) *Alligator* (Fig. 9). It is also apparent this trend is much more pronounced in the large specimen. That this is more related to general trends of CAH (and thus TFT) than to differences in CAH of replacement teeth to CAH of functional teeth can be seen when the relations of the CAH are compared between the upper and lower dentition and the medium and large specimen. In the medium sized specimen the functional tooth's CAH is 3.02 times that of the replacement tooth's CAH

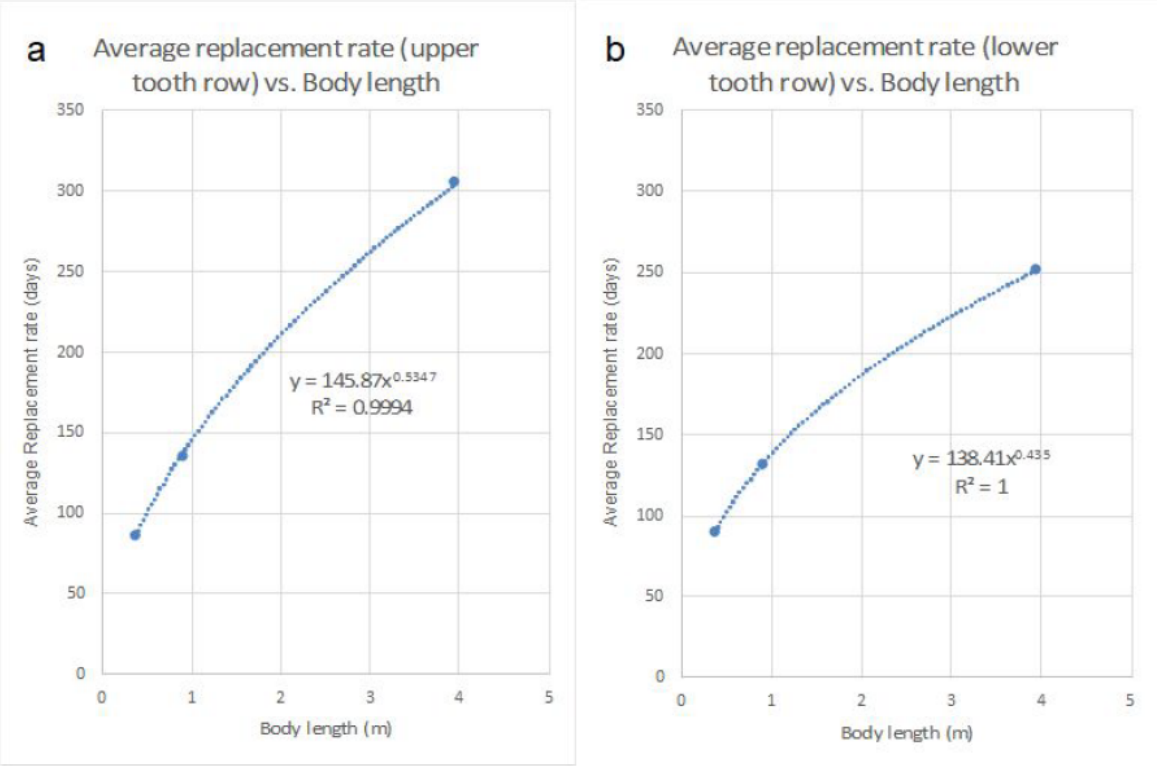

Fig. 9 Tooth Replacement Rate of upper and lower jaw of *Alligator* by Body length
a TRR of the upper tooth row ; **b** TRR of the lower tooth row on the left.

for the upper dentition and 3.07 for the lower dentition. For the large specimen the functional tooth's CAH is 2.66 times that of the replacement tooth's CAH for the upper dentition and 2.73 for the lower dentition. This is a relatively small difference compared to the more than 50 days difference of the average replacement rate in the upper and lower dentition of the large alligator in contrast to the less than 4 days difference of upper and lower replacement rate in the medium sized specimen. However, this perceived difference of upper and lower mandibles and the specimens might be warped by missing functional teeth (and perhaps also replacement teeth) of the large specimen (NCSM 100805). Pmx 4 and Mx 9 are missing in the upper jaw, whereas Dent 1, 3, 17, 18, 19, and 20 are missing in the lower jaw. Whether their presence would have changed this trend or even reinforced it is an open question. In the medium sized specimen the distalmost Dent teeth have comparatively less differences in CAH between functional and replacement teeth.
When those values are further combined to a specimen mean replacement rate the values can be compared to those derived from Erickson (1992). Erickson 1996a adds data points for TRR of hatchling *Alligator* to his Fig. 3 and Erickson 1992 Fig. 13 does the same, both times referring to Westergaard and Ferguson 1990; but this source does not include any notes on the body length of the individuals; thus, those hatchling individuals which in fact anchor the whole lower half of the linear regression were left

out when we entered the additional data from Erickson (1992, 1996a) in Fig. 10. Furthermore when we tried to derive body length and TRR for these two individuals from Fig. 3 in Erickson 1996a and Fig. 13 in Erickson 1992 we arrived at different values for both body length (0.22 m vs. 0.18 m and 0.30 m vs. 0.20 m) and TRR (6.49 vs. 11.41 and 24.74 vs. 20.26) the later of which fall in the continuum of TRRs reported by Westergaard and Ferguson (1990). The values from Erickson (1992) are added to the other data of Erickson and this study in Fig. 11 whereas Fig. 12 does the same for the hatchling values from Erickson (1996).

We see a linear relationship of Body length and TRR in all three variants (Fig. 10, 11, 12). The 2.5 m and 3.2 m long individuals from Erickson (1992) are most removed from the trendline in Fig. 10, but even they are not far off and the fit is relatively good ($R^2 = 0.90$). Adding the hatchling data from Erickson 1992 decreases the fit minimally ($R^2 = 0.886$) but changes the trendline by increasing the slope and lowering the intercept, so that in this version the 2.5 m individual, our 0.906 m long individual, and the smaller of the hatchlings are the most removed from the trendline (Fig. 11). Adding the hatchling data from Erickson 1996 decreases the fit even less ($R^2 = 0.895$) but still changes the trendline by increasing the slope and lowering the intercept, so that in this version the 2.5 m individual, our 0.906 m long individual, and the smaller of the hatchlings are the most removed from the trendline.

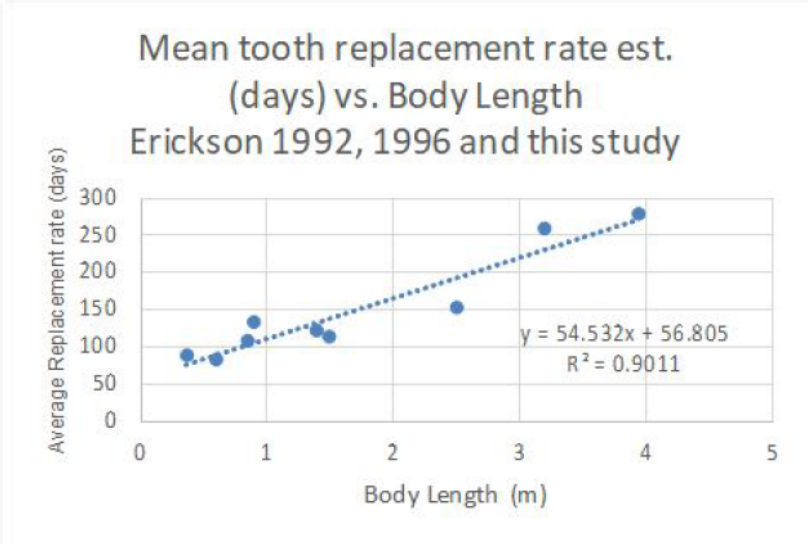

Fig. 10 Mean Tooth Replacement Rate of *Alligator* specimens by Body length

Data from Erickson (1992, 1996) was added to our three specimens to explore the relationship of TRR and Body length. A linear function describes the relationship.

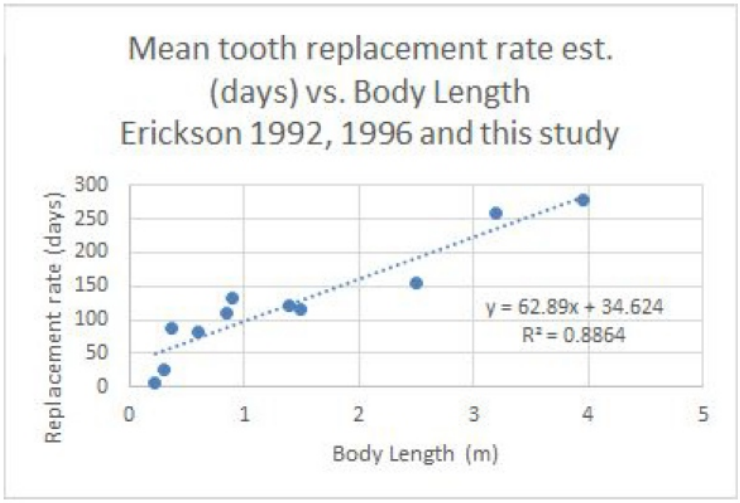

Fig. 11 Mean Tooth Replacement Rate of *Alligator* specimens by Body length withhatchling data from Erickson 1992

Data from Erickson (1992, 1996) was added to our three specimens to explore the relationship of TRR and Body length. A linear function describes the relationship.

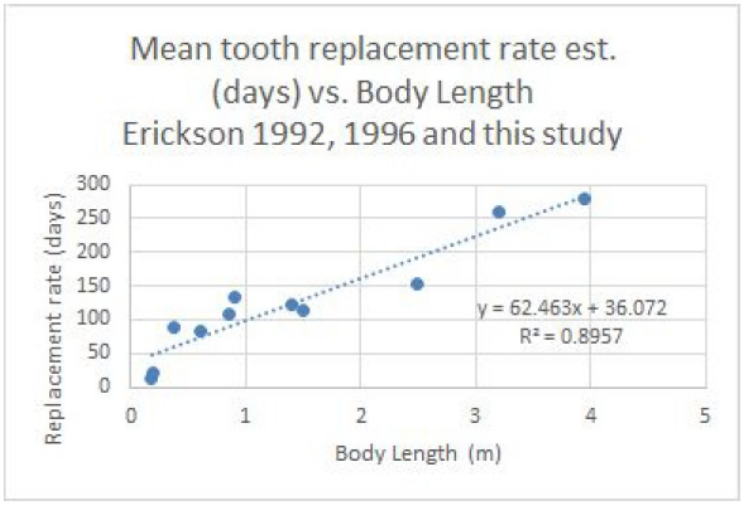

Fig. 12 Mean Tooth Replacement Rate of *Alligator* specimens by Body length withhatchling data from Erickson 1996

Data from Erickson (1992, 1996) was added to our three specimens to explore the relationship of TRR and Body length. A linear function describes the relationship.

Appendix B

crown height [mm]	0.1928	0.2028	0.9228	1.1750	1.2328	1.5628	1.6228	1.6428	1.7850	1.7928	1.8628	2.0528	2.0550	2.0628	2.1328	2.1928	3.4750	4.5650	5.0250	5.2650	5.6550	6.2250	6.4150	8.8250	12.8650	Mean	Variance	t-statistic	p-value
TFT by sampled CA sections [days]	16.0667	17.6348	70.9846	90.3846	70.4457	130.2333	121.7100	131.4240	89.2500	96.9081	128.4690	175.9543	205.5000	134.5304	148.1111	173.1158	133.6538	249.0000	301.5000	195.0000	396.8421	364.0351	342.1333	519.1176	559.3478	194.4541	20739.047		
VEIW of the tooth [mm]	0.0120	0.0115	0.0130	0.0130	0.0175	0.0120	0.0133	0.0125	0.0200	0.0185	0.0145	0.0117	0.0100	0.0153	0.0144	0.0127	0.0260	0.0183	0.0167	0.0270	0.0143	0.0171	0.0188	0.0170	0.0230				
Tooth specific SD [mm]	0.003	0.0025	0.0030	0.0037	0.0048	0.0030	0.0030	0.0028	0.0054	0.004	0.0030	0.0030	0.0020	0.0030	0.0037	0.0030	0.0080	0.0043	0.0035	0.0065	0.0080	0.0110	0.0053	0.0030	0.0050				
TFT (tooth specific SD) + [days]	21.4222	22.5333	92.2800	126.3441	97.0709	173.6444	157.0452	169.3608	122.2603	123.6414	161.9826	236.8615	256.8750	167.2541	199.3271	226.8414	193.0556	325.9938	381.6456	256.8293	904.8000	1020.4918	476.9517	630.3571	714.7222	290.3837	69121.160	1.6001	0.0590
TFT (tooth specific SD) - [days]	12.8533	14.4857	57.6750	70.3593	55.2825	104.1867	99.3551	107.3725	70.2756	79.6800	106.4457	139.9636	171.2500	112.5164	117.8343	139.9660	102.2059	201.4267	249.1736	157.1642	254.1573	221.5302	266.7360	441.2500	459.4643	152.5044	12859.536	-1.1443	0.1293
SD + [days]	5.3556	4.8986	21.2954	35.9595	26.6252	43.4111	35.3352	37.9368	33.0103	26.7333	33.5136	60.9073	51.3750	32.7236	51.2160	53.7256	59.4017	76.9938	80.1456	61.8293	507.9579	656.4567	134.8183	111.2395	155.3744				
SD - [days]	-3.2133	-3.1491	-13.3096	-20.0253	-15.1632	-26.0467	-22.3549	-24.0515	-18.9744	-17.2281	-22.0233	-35.9906	-34.2500	-22.0141	-30.2769	-33.1498	-31.4480	-47.5733	-52.3264	-37.8358	-142.6848	-142.5048	-75.3974	-77.8676	-99.8835				
SD + [%]	33.3333	27.7778	30.0000	39.7849	37.7953	33.3333	29.0323	28.8660	36.9863	27.5862	26.0870	34.6154	25.0000	24.3243	34.5794	31.0345	44.4444	30.9212	26.5823	31.7073	128.0000	180.3279	39.4052	21.4286	27.7778				
SD - [%]	-20.0000	-17.8571	-18.7500	-22.1557	-21.5247	-20.0000	-18.3673	-18.3007	-21.2598	-17.7778	-17.1429	-20.4545	-16.6667	-16.3636	-20.4420	-19.1489	-23.5294	-19.1058	-17.3554	-19.4030	-35.9551	-39.1459	-22.0374	-15.0000	-17.8571				

Table 1TFTs with upper and lower SD range using the tooth specific SDs
TFTs based on mean VEIWs for the sampled tooth positions sorted by ascending CAH. Rows TFT ± SD show the TFT based on VEIW ± SD derived from the that tooth. TFT+ SD shows the mean VEIW [tooth] - 1 SD [tooth] (TFT+ SD, as it produces bigger TFTs); TFT- SD shows VEIW [tooth] + 1 SD [tooth] (TFT- SD as it produces smaller TFTs). SD ± [days] show the differences of TFT ± SD to the baseline TFT. Rows SD ± [%] are showing the same differences in percent (see also S2, Fig 1). The last four columns show the mean TFT, the variance, t-test statistic and the p-value for a one sided two sample t-test comparing the upper and lower TFT ranges based on the mean SD of VEIWs.

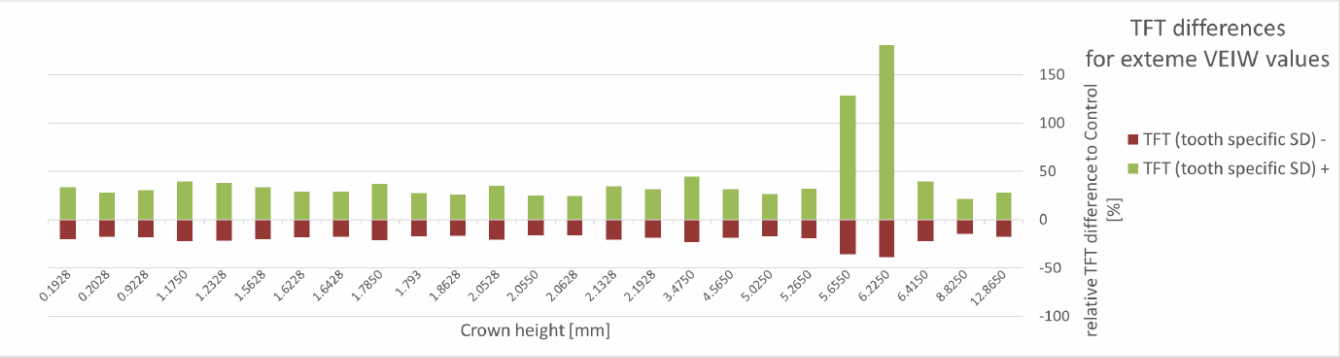

Figure 1 TFT differences for extreme VEIW values using tooth specific SDs
For each tooth (on the x-axis with their crown height) the deviation of the upper and lower TFT estimate (upper estimate: based on mean VEIW [tooth] - 1 SD [tooth]; lower estimate based on mean VEIW [tooth] + 1 SD [tooth]) to the calculated TFTs [based on mean VEIW [tooth]) is shown in percent (see last two rows of table 4). Lower TFT estimates are in red-brown, upper TFT estimates in green.

Note on Appendix C

Sampling Impacts the Assessment of Tooth Growth and Replacement Rates in Archosaurs Suppl appendix C is an Excel file. It is available for download on the NC State library repository page where this thesis can be found as well.